Target-dependent suppression of siRNA production modulates the levels of endogenous siRNAs in *C. elegans* germline

Zoran Gajic[1,*,¶], Diljeet Kaur[1,‡,¶], Julie Ni[1,¶], Zhaorong Zhu[1], Anna Zhebrun[1], Maria Gajic[1], Matthew Kim[1,§], Julia Hong[1], Monika Priyadarshini[2], Christian Frøkjær-Jensen[2], Sam Gu[1,**]

[1]Department of Molecular Biology and Biochemistry, Rutgers, The State University of New Jersey, Piscataway, NJ 08854, USA

[2]Biological and Environmental Sciences and Engineering Division (BESE), King Abdullah University of Science and Technology (KAUST), Thuwal 23955–6900, Kingdom of Saudi Arabia

[*]Present address: Vilcek Institute of Graduate Biomedical Sciences, NYU Langone Health, New York, NY 10010, USA.

[‡]Present address: Genetics and Epigenetics Program, The University of Pennsylvania, Philadelphia, PA 19104, USA.

[§]Present address: University of Pennsylvania, Philadelphia, PA 19104, USA.

[¶]These authors contributed equally to this work

[**]Author for correspondence: sam.gu@rutgers.edu

Key words: siRNA suppression, genome surveillance, C. elegans germline, RNAi, transposon

Summary statement:

Target-dependent suppression of siRNA production helps distinguishing self vs nonself siRNAs in *C. elegans germline* and adds complexity to the RNAi-mediated epigenetics.

Abstract

Despite the prominent role of endo-siRNAs in transposon silencing, their expression is not limited to these “nonself” DNA elements. Transcripts of protein-coding genes (“self” DNA) in some cases also produce endo-siRNAs in yeast, plants, and animals (Piatek and Werner 2014). How cells distinguish these two populations of siRNAs to prevent unwanted silencing of active genes in animals is not well understood. To address this question, we inserted various self-gene or gfp fragments into an LTR retrotransposon that produces abundant siRNAs and examined the propensity of these gene fragments to produce ectopic siRNAs in *C. elegans* germline. We found that fragments of germline genes are generally protected from production of ectopic siRNAs. This phenomenon, which we termed “target-

directed suppression of siRNA production" (or siRNA suppression), is dependent on the germline expression of target mRNA and requires germline P-granule components. We found that siRNA suppression can also occur to naturally produced endo-siRNAs. We suggest that siRNA suppression plays an important role in regulating siRNA expression and preventing self-genes from aberrant epigenetic silencing.

Introduction

Small RNAs, such as microRNAs, endo-siRNAs, and piRNAs carry out a diverse set of cellular functions through their ability to silence homologous genes. Small RNAs orchestrate gene silencing by serving as guide molecules to bring Argonaute and other regulatory proteins to the target RNA transcripts. Therefore, the steady state level of small RNAs is a key determinant of the gene silencing activity.

The endo-siRNA pathway in *C. elegans* germline is a powerful system to explore small RNA biology and transgenerational epigenetic inheritance (Billi, Fischer et al. 2014). Among the different classes of endo-siRNAs, the ones that target transposons and other repetitive DNA elements belong to secondary siRNA or 22G-RNA class (Gu, Shirayama et al. 2009), which are *de-novo* synthesized by RNA-dependent RNA polymerases (RdRPs) using the target mRNAs as the template. 22G-RNA synthesis can be triggered by a diverse set of RNA molecules/structures: dsRNA (Fire, Xu et al. 1998), 26G-RNA (Han, Manoharan et al. 2009, Gent, Lamm et al. 2010), piRNA (Ashe, Sapetschnig et al. 2012, Lee, Gu et al. 2012), aberrant mRNA processing (Newman, Ji et al. 2018, Makeyeva, Shirayama et al. 2021), and untemplated RNA-tailing (Shukla, Yan et al. 2020) . Once produced, these siRNAs are bound by the germline AGO proteins such as WAGO-1 (Gu, Shirayama et al. 2009) and HRDE-1 (Buckley, Burkhart et al. 2012), which induce post-transcriptional and transcriptional repression at the target genes. The steady state level of siRNAs is determined through both biogenesis and turnover of siRNAs. Recent studies have identified numerous biochemical activities that can affect the siRNA turnover rate, such as siRNA tailing (van Wolfswinkel, Claycomb et al. 2009, Pisacane and Halic 2017, Zhou, Feng et al. 2017, Wang, Weng et al. 2020) and the stability and processing of AGO proteins (Batista, Ruby et al. 2008, Gudipati, Braun et al. 2021). In these cases, it is unclear to what extent the siRNA turnover is mediated by their target mRNA.

Interestingly, actively transcribed germline genes also naturally produce 22G-class siRNAs in *C. elegans* (Claycomb, Batista et al. 2009, Maniar and Fire 2011). For the purpose of this study, we refer to these siRNAs as self siRNAs and the ones from transposons as nonself siRNAs. Both populations are synthesized by RdRPs and share the same size distribution that peaks at 22 nt and the 5' guanine bias. Despite these similarities, the self siRNAs differ from the nonself siRNAs in at least two aspects. First, self siRNAs have much lower density, as measured by normalized read count per unit length of mRNA, than nonself siRNAs (Fig. S1). Second, they are enriched in different AGO proteins: the nonself siRNAs in WAGO-1 and HRDE-1 and self siRNAs in another germline-specific AGO protein CSR-1 (Claycomb, Batista et al. 2009). Self siRNAs have been suggested to fine-tune germline gene expression: loss of the germline RdRP enzyme EGO-1 leads to reduced levels of self siRNAs and increased mRNA expressions of the corresponding germline genes (Maniar and Fire 2011); loss of the CSR-1 protein also led to complex dysregulation of germline gene expression and ultimately sterility (Claycomb, Batista et al. 2009, Seth,

Shirayama et al. 2013, Cecere, Hoersch et al. 2014, Campbell and Updike 2015, Gerson-Gurwitz, Wang et al. 2016, Fassnacht, Tocchini et al. 2018).

Despite the clear distinctions in their abundance and biochemical properties, how cells distinguish the self and nonself siRNAs remains largely unknown. Transposons and self genes differ significantly in their chromatin environment, modes of transcription, RNA processing and trafficking, which can all potentially affect siRNA production and loading into AGOs. However, it is hard to change one factor without affecting other, which makes it difficult to interpret the results obtained from using mutants of in the aforementioned pathways. In this study, we took a genome engineering approach to insert various self-gene and gfp DNA fragments into an LTR retrotransposon *Cer3*, which is a natural "hot spot" of nonself siRNAs. This enables us to examine the propensity of self-gene fragments in producing siRNAs when embedded in a nonself siRNA-producing genomic environment.

Results:

The design of ectopic siRNA production from the LTR retrotransposon *Cer3*

In this study we used CRISPR to insert approximately 400 nt exonic sequences from various protein-coding genes into the LTR retrotransposon *Cer3* to test whether the protein coding gene fragments produce ectopic siRNAs (Fig. 1A). *Cer3* is a native target of germline nuclear RNAi and produces abundant germline-specific siRNAs (Fig. 1B, S1A, S2) (Ni, Chen et al. 2014, Ni, Kalinava et al. 2018). There is only one copy of *Cer3* in the genome of the wild-type Bristol N2 strain. The insertion site was chosen for its local peak level of siRNA production (Fig. S2). Single nucleotide polymorphisms (SNPs) were introduced in some of the insertions at 30 nt intervals to distinguish between the transposon-driven ectopic siRNAs and the native self siRNAs (generated from the homologous target genes).

Suppression of *Cer3*-driven ectopic siRNAs against germline genes

Synchronized young adults carrying various *Cer3::insertion* mutations were subject for sRNA-seq analysis. We found that none of the insertions used in this study affected the *Cer3* siRNA expression (Fig. 1 and S3). However, the levels of the ectopic siRNAs from different insertions varied significantly. Insertions of a *gfp* fragment (*Cer3::gfp*) (Fig. 1F) and four somatic gene fragments (*ida-1, ttm-2, cah-4, and unc-22,* selected for preferentially neuronal, intestinal, hypodermal, or muscle expression, respectively, based on RNA-seq data from (Serizay, Dong et al. 2020)) (Fig. 1C, Fig. S4A-C) produced abundant siRNAs, with levels similar to the ones expressed from the flanking *Cer3* sequences (Fig. 1J). In contrast, fragments from four germline-expressed genes (*oma-1, zim-3, him-5,* and *mex-5*) and one ubiquitously expressed ribosomal protein gene (*rpl-1*) produced significantly fewer siRNAs than the flanking *Cer3* siRNAs (Figs. 1D-E, S4D-E, S4G, 1J). We also crossed the *Cer3:gfp* allele into strains that carry a germline-expressed *gfp* transgene, either a translational fusion of *oma-1::gfp* or *gfp* driven by a germline-specific promoter (*Pmex-5::oma-1*). We found that the *Cer3*-driven *gfp* siRNAs were produced in much lower abundance in both the *gfp* transgene (+) animals than in the *gfp* transgene (-) animals (Fig. 1G and H). In total, we tested nine strains in which germline-expressed fragments were inserted into *Cer3.* While most of the *Cer3::insertion* containing germline gene fragments exhibited suppressed level of siRNAs produced from the insertions (Fig. 1D-E, 1G-H, S4D-G), we did observed two exceptions

from the *Cer3::meg-2* (Fig. 1I) and *Cer3::him-8* (Fig. S4F) which produced abundant siRNAs from the insertions. We do not know the reason for these exceptions at this point (some speculations were given in Discussion).

To compare the relative expression of siRNAs from *Cer3* and insertions, we defined an siRNA suppression index (SSI) as the ratio between the density of flanking *Cer3* siRNAs and insertion siRNAs. The average SSI for the germline-expressed fragments (except *him-8* and *meg-2*) fragments was 4.5. In contrast, the average SSI for *gfp* (WT background) and somatic fragments is 0.8. We also inserted the *oma-1* fragment into a different LTR retrotransposon *Cer8* and observed a similar suppressive effect on the production of the ectopic *oma-1* siRNAs (Fig. S4 H and I). These results indicate that germline-expressed gene fragments tend to be protected from siRNA production even when embedded in siRNA hotspots such as in transposon sequences. We refer to this phenomenon as "siRNA suppression" in this paper. The germline gene *oma-1* has been extensively used as a native gene to study RNAi and transgenerational epigenetic silencing (Alcazar, Lin et al. 2008). For the rest of the study, we used the *Cer3::oma-1* allele to characterize siRNA suppression.

The siRNA suppression effect is local and limited to the homologous sequence

We found that siRNA suppression did not spread to either side of the flanking *Cer3* sequences (Fig. 1 B, D, G, H and Fig. S3 A, C), suggesting that the siRNA suppression effect is local. To further test the local effect, we reduced the length of the sequence homology by deleting a 240 bp segment from the *oma-1* gene in the strain that carried the same *Cer3::oma-1* allele as used in Fig. 1D. The deleted sequence matches fragment B of *Cer3::oma-1* as indicated in Fig. 2A, leaving fragment A as the only sequence in *Cer3::oma-1* with homology to the mutant *oma-1*. We found that the *oma-1* deletion abrogated the siRNA suppression for fragment B, but not for fragment A (Fig. 2A). This result confirms that (1) the siRNA suppression requires the homologous DNA sequence in the target gene and (2) the suppression is highly local and does not spread to flanking non-homologous sequence in *Cer3*.

siRNA suppression is likely mediated by mRNA

We hypothesized that siRNA suppression is mediated by the target mRNA and thus tested the requirement of promoter, strand specificity, and the effect of mRNA silencing on siRNA suppression.

One way to abolish *oma-1* transcription is to delete the *oma-1* promoter. Our attempt on this using CRISPR was unsuccessful, so we used the available *oma-1[tm1396]* allele (Consortium 2012), which deletes a 1.5 kb sequence including the promoter and a large fraction of the transcribed sequence of *oma-1*, including part (232 bp) of the homologous sequence to *Cer3::oma-1* (Fig. 2B). In the remaining *oma-1* sequence, 187 bp still shares sequence homology to *Cer3::oma-1* (fragment C in Fig. 2B). We found that this *oma-1* mutation abrogated the siRNA suppression effect for the entire *oma-1* insertion of *Cer3::oma-1*, including fragment C (Fig. 2B), suggesting that the *oma-1* promoter is required for siRNA suppression.

To test the strand specificity, we compared two *Cer3::oma-1* alleles that differ in the orientation of the *oma-1* insertion, with one producing antisense *oma-1* siRNAs (Fig. 1D) and the other sense *oma-1* siRNAs (Fig. 2C). We found that, unlike the antisense *oma-1* siRNAs, sense *oma-1* siRNAs were not suppressed (Fig. 2C). Therefore, the siRNA suppression effect is specific to antisense siRNAs.

To test the effect of *oma-1* mRNA silencing on siRNA suppression, we first performed *oma-1* RNAi by feeding worms with dsRNA that targets a sequence upstream to the homologous sequence to *Cer3::oma-1* (Fig. S5A). We found that the siRNA suppression was not affected (Fig. S5A). We then performed a piRNA-triggered *oma-1* silencing (piRNAi) using a piRNA-expressing transgene approach recently developed in (Priyadarshini, Ni et al. 2022). The target sites of the six artificial piRNAs spread along the *oma-1* gene (Fig. S6A). Consistent with the previous report (Priyadarshini, Ni et al. 2022), our RNA-seq analysis indicated that piRNAi induced a much more robust *oma-1* silencing (29.1-fold) than dsRNA (4.6-fold) (Fig. S5B and C). Two piRNA sites also fall into the *oma-1* sequence in *Cer3::oma-1* (Fig. S6A), therefore may directly impact siRNA production from *Cer3::oma-1.* To rule out this possibility, we also generated a new *Cer3::oma-1* allele (red118) that deleted the two piRNA sites, but otherwise is identical to the allele (red20) that was frequently used in this study (Fig. S6A). We found that *oma-1* piRNAi abrogated the siRNA suppression for both alleles of *Cer3::oma-1* (Fig. 2D and S6A), while the control samples of *unc-119* piRNAi (Fig. 2E) or no piRNAi (Fig. S6B) exhibited strong siRNA suppression at *Cer3::oma-1*. These results suggest that siRNA suppression can be reversed by a strong silencing of the target gene (by piRNAi). Because siRNA suppression is not affected by a more modest silencing effect of the target gene (by dsRNA), we suggest that the amount of mRNA needed for siRNA suppression can be low.

Taken together, our results shown in this section strongly suggest that siRNA suppression is mediated by the mRNA of the homologous germline gene.

siRNA suppression does not require the germline AGO proteins HRDE-1, CSR-1, or the piRNA pathway, but requires the P-granule components

We then performed a small scale candidate gene-based screen to investigate the genetic requirement of siRNA suppression using *Cer3::oma-1*. CSR-1 and HRDE-1 are two germline-specific AGO proteins that preferentially bind different populations of germline siRNAs: self siRNAs for CSR-1 and nonself siRNAs for HRDE-1 (Claycomb, Batista et al. 2009, Ashe, Sapetschnig et al. 2012, Buckley, Burkhart et al. 2012, Shirayama, Seth et al. 2012). We found that neither the *hrde-1(-)* mutation nor CSR-1 depletion by auxin-induced protein degradation (AID) affected the siRNA suppression of *Cer3::oma-1* (Fig. 3B-C, 3I, S7), indicating that HRDE-1 and CSR-1 are not required for siRNA suppression in adult animals. In our experiment, CSR-1 depletion occurred continuously from the embryo to the adult stage. Consistent with the published work (Claycomb, Batista et al. 2009), CSR-1 depletion caused a complete embryonic lethal phenotype (data not shown), which prevented us to examine any intra- or inter-generational impact on siRNA suppression. Therefore, we cannot rule out the possibility that CSR-1 promotes the establishment of the siRNA suppression either in the early embryo or in the previous generation but is not required for the maintenance of siRNA suppression in adults.

Recent studies have shown that the piRNA pathway can suppress the run-away siRNA amplification in *C. elegans* (Shukla, Yan et al. 2020, Montgomery, Vijayasarathy et al. 2021, Wahba, Hansen et al. 2021). The PRDE-1 protein is required for the biogenesis of piRNAs (Kasper, Wang et al. 2014, Weick, Sarkies et al. 2014) and PRG-1 is the PIWI protein that binds piRNAs (Batista, Ruby et al. 2008); both are essential for the piRNA-mediated functions (Billi, Fischer et al. 2014). We observed strong siRNA suppression of *Cer3::oma-1* in the *prg-1(-)* and *prde-1(-)* animals (Fig. 3D-E, 3I), indicating that piRNA activity is not required for siRNA suppression of *Cer3::oma-1*.

The P granules in *C. elegans* germline are liquid-like, membrane-less condensates of RNA and proteins, that often locate adjacent to the cytoplasmic side of the nuclear pore complexes (Strome and Wood 1982). Many proteins in the RNAi pathway are enriched in the P granules, and the P granules have been shown to promote RNAi (Seydoux 2018, Marnik and Updike 2019). Consistent with this notion, we found that mutant animals lacking any of the P-granule assembly factors DEPS-1, GLH-1, and PGL-1 showed reduced levels of *Cer3* siRNAs (Fig. S8). We crossed the *Cer3::oma-1* allele into these P-granule mutants. We sequenced deeper for these samples in order to obtain sufficient siRNA reads to quantify siRNA suppression at *Cer3::oma-1*. We found that the siRNA suppression effect was abrogated in *deps-1(-)* and *glh-1(-)* animals (Fig. 3F-G). The *pgl-1(-)* mutation also weakened the siRNA suppression effect albeit to a lesser degree than *deps-1(-)* or *glh-1(-)* (Fig. 3H). These results suggest that siRNA suppression requires functional P granules.

Unsuppressed ectopic siRNAs induce transitive RNAi of the target gene

To determine the impact of *Cer3*-driven ectopic siRNAs on the target gene mRNA expression, we performed RT-qPCR analyses of the corresponding target genes in worms carrying the *Cer3::oma-1*, *Cer3::zim-3*, *Cer3::rpl-1* or *Cer3::meg-2* alleles. For the *Cer3::oma-1*, *Cer3::zim-3*, and *Cer3::rpl-1* alleles, which all exhibited strong siRNA suppression, their corresponding target gene mRNAs were expressed at the wild-type level (Fig. 4 A-C), and their overall siRNA levels, as well as the relative siRNA distribution along the gene body, were not affected (Fig. 4E-G and I-K), indicating a lack of RNAi at these genes. In contrast, *Cer3::meg-2*, which is resistant to siRNA suppression, was associated with a 43% reduction in *meg-2* mRNA (Fig. 4D) and a 28-fold increase in *meg-2* siRNAs (Fig. 4H), with the most prominent siRNA increase at the region homologous to the inserted sequence in *Cer3::meg-2* (Fig. 4L). These results indicate that the *Cer3*-driven ectopic siRNAs, if not suppressed, can induce a transitive RNAi effect at the target gene.

siRNA suppression of the native siRNAs

So far, our experiments only examined ectopic siRNAs expressed from genetically engineered loci. We next wished to determine whether the native nonself siRNA can be suppressed by an increased level of homologous mRNA. We took two different approaches to increase the level of the homologous mRNA.

First, we inserted a 467 nt *Cer3* fragment in the 3' UTR of the native *oma-1* gene (*oma-1::Cer3*) (Fig. 5A) and examined its impact on siRNA expressions of *oma-1* and *Cer3*. The *Cer3* fragment was chosen for its high siRNA expression in *Cer3*. Although the *Cer3* insertion produced more siRNAs than

the flanking *oma-1* sequence (Fig. S9A), it did not significantly affect the expressions of *oma-1* mRNA or siRNA (Fig. S9B-C). However, the *oma-1::Cer3* mutant animals exhibited a striking suppression of siRNA production in *Cer3*. Like the cases mentioned earlier, the siRNA suppression effect was specific to the homologous sequence without spreading to the adjacent *Cer3* sequence (Fig. 5A-B and Fig. S9D).

In our second experiment, we asked whether *hrde-1* mutation can lead to siRNA suppression at the desilenced native HRDE-1 targets. To this end, we analyzed our previously published mRNA-seq and sRNA-seq data of the WT and *hrde-1*(-) animals cultured at 23°C (Ni, Kalinava et al. 2016). Out of the top 20 desilenced genes in the *hrde-1(-)* mutant (>16-fold desilencing, $p<0.05$) (Fig. 5C), 12 genes had at least 3-fold decreases in siRNA expression ($p<0.05$) (Fig. 5D). Such association supports the idea that desilencing of the native HRDE-1 targets leads to suppression of siRNA production. However, certain AGO proteins (e.g. PRG-1 (Batista, Ruby et al. 2008)) have been shown to promote the stability of the bound small RNAs. For this reason, we also examined the *nrde-2* mutant. NRDE-2 is an effector nuclear RNAi factor, functioning downstream to the siRNA production, and itself is not an AGO protein (Guang, Bochner et al. 2010). Therefore, the loss of NRDE-2 is unlikely to have any direct impact on the siRNA biogenesis or turnover. Similar to *hrde-1*, *nrde-2* mutation also caused losses of siRNAs at the desilenced native HRDE-1 targets (Fig. 5E-G), which further supports that desilencing of the native HRDE-1 targets can suppress the production of the targeting siRNAs.

Taken together, these results indicate that siRNA suppression is not limited to genetically engineered ectopic siRNAs, but can also occur to native siRNAs when the homologous mRNA sequence is actively expressed *in cis* or *in trans*.

Cer3-driven ectopic siRNAs are preferentially loaded in HRDE-1 over CSR-1

As mentioned earlier, HRDE-1 prefers to bind nonself siRNAs and CSR-1 prefers to bind self siRNAs. We wished to determine whether the *Cer3*-driven ectopic siRNAs are preferentially loaded into HRDE-1 or CSR-1. To this end, we generated a strain that expresses *Cer3::oma-1*, SF(strep II-FLAG)-HRDE-1, and c-myc-CSR-1 and sequenced the HRDE-1-bound siRNAs and CSR-1-bound siRNAs by the small RNA co-immunoprecipitation (sRIP)-seq experiment. The relative HRDE-1 or CSR-1 preference was measured by the ratio of sRIP-seq signal (HRDE-1 or CSR-1 IP, respectively) over the input signal. We first confirmed that siRNAs from known HRDE-1 targets, such as *Cer3*, *bath-45*, and *f15d4.5,* were much more enriched in the HRDE-1 coIP siRNAs than the CSR-1 ones (Fig. 6). In contrast, germline genes such as *oma-1*, *prg-1*, and *pgl-1* showed higher relative enrichment in CSR-1 than in HRDE-1 (Fig. 6), as expected. Similar to the *Cer3* siRNAs, the ectopic *oma-1* siRNAs from *Cer3::oma-1* showed a much higher enrichment in HRDE-1 than in CSR-1 (Fig. 6), indicating a strong preference of HRDE-1 over CSR-1 for *Cer3*-driven ectopic siRNAs.

Discussion

One paradox of RNAi is that the mRNAs are both the target and a necessary component of RNAi for mRNAs are the substrates or templates for siRNA biogenesis. Here we showed that the target transcripts can also suppress the homologous siRNAs. This further increases the complexity in the mRNA-siRNA relationship and epigenetic regulation in *C. elegans* germline (Fig. 7). We suggest that,

nonself DNA such as transposons are active in producing endo-siRNAs, but inactive in siRNA suppression due to the low level of their mRNAs. The germline expressed genes (self DNA) are the opposite: relatively low activity in siRNA biogenesis but high activity in siRNA suppression due to the high level of mRNAs. Previous studies have shown that factors that promote siRNA turnover play a key role in preventing unwanted silencing in the genome (van Wolfswinkel, Claycomb et al. 2009, Pisacane and Halic 2017, Zhou, Feng et al. 2017, Wang, Weng et al. 2020). In these cases, it was unclear to what extent the siRNA turnover was dependent on the target mRNA. Our study demonstrates that target-dependent suppression of siRNA production is an integral component of the RNAi pathway in *C. elegans* germline and plays an important role in distinguishing self and nonself genetic material.

Potential biological functions

RNAi in *C. elegans* germline is highly robust and long-lasting (Fire, Xu et al. 1998, Grishok, Tabara et al. 2000, Vastenhouw, Brunschwig et al. 2006, Alcazar, Lin et al. 2008, Devanapally, Raman et al. 2021). These features, while essential for genome surveillance against nonself DNA, can potentially lead to unwanted silencing of self genes. Previous studies have shown that epimutations of self genes can be induced by a diverse set of experimental triggers and genetic conditions (Johnson and Spence 2011, Ashe, Sapetschnig et al. 2012, de Albuquerque, Placentino et al. 2015, Phillips, Brown et al. 2015, Shukla, Yan et al. 2020, Montgomery, Vijayasarathy et al. 2021, Wahba, Hansen et al. 2021). The risk of epimutation is further increased by the presence of the siRNAs that are naturally produced from germline genes. For example, rRNA genes appear to be particularly prone to aberrant siRNA production and silencing (Zhou, Feng et al. 2017, Reed, Svendsen et al. 2020, Montgomery, Vijayasarathy et al. 2021, Wahba, Hansen et al. 2021). Some active genes contain siRNA-producing transposon elements in their introns or nearby intergenic regions. In addition, a recent epimutation accumulation study found that siRNAs can increase for certain self-genes in wild type populations (Beltran, Shahrezaei et al. 2020). Interestingly, such increases appear to be transient. These observations highlight the importance of regulating self-targeting siRNAs.

The aberrant RNAi of self genes is likely to be prevented by multiple mechanisms. The lack of silencing triggers, such as dsRNA, piRNA, 26G-RNA, pUG or other untemplated tails, is likely the major reason for the absence or low level of siRNAs from self genes (Billi, Fischer et al. 2014). The target-dependent siRNA suppression can provide another mechanism against unwanted silencing by distinguishing the self and nonself siRNAs. Given the large difference in the mRNA levels between the self and nonself genes, the dependance on the target mRNA can ensure the specificity of self-siRNA suppression and avoid suppressing the nonself siRNAs. Target-directed siRNA suppression may also contribute to the previously observed non-coding function of mRNA in promoting gene expression (Johnson and Spence 2011, Seth, Shirayama et al. 2013, Seth, Shirayama et al. 2018, Devanapally, Raman et al. 2021). We note that target-directed siRNA suppression did not completely abolish ectopic siRNAs. Rather this feature is perhaps important for the fine tuning the siRNA levels of germline genes.

Mechanistic considerations

siRNA synthesis or degradation? In principle, there are two ways to achieve target-directed siRNA suppression: inhibiting siRNA biogenesis or enhancing siRNA turnover. At this point we find it difficult to imagine how target mRNAs *directly* inhibit the synthesis of ectopic siRNA synthesis. siRNAs produced

from the target mRNA, on the other hand, can potentially bind to the homologous RNA sequence inserted in *Cer3*, and function as a barrier against the RdRP activity, as suggested by (Shen, Chen et al. 2018). However, such model would predict that the *Cer3* siRNAs that are immediately upstream to the insertion would be suppressed as well. We did not observe such effect. Instead, the siRNA suppression was highly limited to the homologous sequence. Although we cannot rule out a model involving siRNA synthesis inhibition, we currently favor a target mRNA-mediated siRNA degradation model, perhaps using a mechanism that is similar to target-dependent microRNA degradation (Ameres, Horwich et al. 2010, Sheu-Gruttadauria, Pawlica et al. 2019) or RNA tailing mediated sRNA degradation (van Wolfswinkel, Claycomb et al. 2009, Pisacane and Halic 2017, Zhou, Feng et al. 2017, Wang, Weng et al. 2020, Yang, Shao et al. 2020). In addition, the steady state level of siRNAs can also be affected by activities that influence the Argonaute proteins' ability to bind siRNAs (Gudipati, Braun et al. 2021). We did not observe any above-background level of tailing for *Cer3*-driven ectopic siRNAs (data not shown), but we cannot rule out the possibility of rapid siRNA degradation after tailing. Recent studies have shown that the piRNA pathway, in addition to its silencing role, protect the rRNA locus, histones, and other self genes from aberrant siRNA production and silencing (Shukla, Yan et al. 2020, Montgomery, Vijayasarathy et al. 2021, Wahba, Hansen et al. 2021, Priyadarshini, Ni et al. 2022). Future studies are needed to determine to what extend these activities are directed by target RNA.

P granules. We found that loss of P-granule components GLH-1, DEPS-1, or PGL-1 leads to siRNA suppression defect. Future studies are needed to test whether siRNA suppression occurs in the P granules. Such possibility is intriguing in that the P granules and other adjacent paranuclear condensates have been suggested as a hub for siRNA production and mRNA aggregation (Seydoux 2018). The close proximity of siRNA biogenesis and siRNA suppression could reduce the chance of the unwanted siRNAs escaping from the quality control mechanism. One complication is that mutations in *glh-1, deps-1*, and *pgl-1* also reduce endo-siRNA production at *Cer3* and elsewhere, which compromises the utility of these mutants in studying the function of siRNA suppression.

The exceptions. Our study showed that the germline expression of the target mRNA is a necessary factor but not a sufficient determinant in siRNA suppression. Additional factors can be chromatin marks, modes of transcriptional and post-transcriptional regulation, sub-cellular localization of mRNAs, and levels and Argonaut preference of endo-siRNAs. Future studies are needed to identify additional rules of siRNA suppression.

We suggest that the target-dependent suppression of siRNA production may distinguish self and nonself siRNA and play additional functions in other eukaryotes. We also note that such activity should be considered in mRNA-based technology and therapy.

Methods and Material:

***C. elegans* culture**

C. elegans were cultured at 20°C on NGM plates seeded with *E. coli* OP50 as described in (Brenner 1974) unless indicated otherwise. Synchronized young adult animals, prepared as described in (Ni, Kalinava et al. 2016), were used for all experiments in this study.

CRISPR

CRISPR experiments were conducted using protocols described in (Arribere, Bell et al. 2014, Paix, Folkmann et al. 2015). Briefly, the injection mix generally consists of 1 µg/µl Cas9 (IDT), 2.5 µM *dpy-10* sgRNA (Synthego), 0.4 µM ssDNA oligo as *dpy-10* [*cn64*] repair template, 10 µM target sgRNA, target repair template DNA (2 µM for ssDNA oligo or 0.4 µM for dsDNA with single-stranded overhangs generated using a method described in (Dokshin, Ghanta et al. 2018)). All CRISPR-generated mutations were confirmed by Sanger sequencing.

Design of the Cer3-based siRNA generator

An approximately 400 nt cDNA sequence from *C. elegans* protein-coding genes or gfp was inserted into *Cer3* between base positions 914,783 and 914,784 of chromosome IV (WS190). Single-nucleotide mismatches separated by 30 nt intervals were introduced to the inserted sequence to distinguish siRNAs produced from the *Cer3::insertion* locus and ones from native genes.

Small RNA library preparation and sequencing

Small RNA extraction was performed using the MirVana kit (Thermo Fisher). Small RNA libraries were constructed using the 5'-mono-phosphate-independent, linker ligation-based method as described in (Ni, Kalinava et al. 2016). A mixture of barcodes (set 1: AGCG, CGTC, GTTA, and TATG; set 2: CTGG, ACTG, GAAG, and TGCC) were added to the 5' end of small RNA for each library, as indicated in the meta data file deposited in NCBI GEO database. The standard Illumina Hi-seq indexes (8 nt) were added at the PCR step to allow multiplexing. The libraries were pooled and sequenced on the Illumina HiSeq instrument.

HRDE-1 and CSR-1 sRIP-seq

HRDE-1 and CSR-1 were endogenously tagged at their N-termini with the Strep-tag II-FLAG tag (DYKDDDDKGSAASWSHPQFEKGGGSGGGSGGGSWSHPQFEK) (Ni, Kalinava et al. 2018) (Gloeckner, Boldt et al. 2009) and the c-myc tag (EQKLISEEDL), respectively. CSR-1 has two isoforms (F20D12.1a and F20D12.1b). The c-myc was tagged to the N-terminus of the shorter isoform F20D12.1b, which is constitutively expressed in the germline (Charlesworth, Seroussi et al. 2021). *Cer3::oma-1;sf-hrde-1;c-myc-csr-1* adult animals were used for the sRIP experiment. Cells were lysed by grinding the worms in liquid nitrogen with mortar and pestle.

HRDE-1 IP was performed using FLAG Immunoprecipitation kit (Sigma FLAGIPT1-1KT). Briefly, each worm grind (~5000 young adults pulverize in liquid nitrogen) was lysed in 1ml lysis buffer (Sigma FLAGIPT1-1KT) with 10 µl of HALT protease inhibitor cocktail (ThermoFisher) and 10 µl of RNAaseIn (Promega) at room temperature on a rotator for 15 minutes. Because HRDE-1 is a nuclear protein and might be chromatin bound, the crude lyate was sonicated using a Bioruptor (Diagenode) for 7.5 minutes and three times at 4 °C (setting: high, 30 sec on and 30 sec off). The lysis was clarified by centrifuging at 14,000g for 4 minutes at 4 °C, and the lysis supernatant was collected and was used as IP input. The lysis supernatant was incubated with 40 µl of ANTI-FLAG M2 gel resin at 4 °C overnight. And then the resin was washed three times in 1xWash Buffer (Sigma FLAGIPT1-1KT). The FLAG-tagged protein was eluted by competing with 150 µg/ul 3xFLAG peptide at 4 °C for 30 minutes.

CSR-1 IP was performed using Pierce Magnetic c-Myc-Tag IP/Co-IP kit (ThermoFisher). Each worm grind (~5000 young adults pulverize in liquid nitrogen) was lysed in 1ml Buffer-1 with 10 µl of HALT protease inhibitor cocktail (ThermoFisher) and 10 µl of RNAaseIn (Promega) at room temperature on a rotator for 5 minutes. The lysis was clarified by spinning at 14,000g for 10 mins at 4 °C. The lysis supernatant was used as IP input. The lysis supernatant was incubated with 25 µl of pre-washed anti-cMyc meganetic beads at room temperature for 30 minutes. And then the beads were washed three times with 300 µl 1xBuffer-2. The cMyc-tagged protein was eluted by 0.5mg/ml cMyc peptide in elution buffer at 37°C for 5 minutes. Western blotting was used to validate the HRDE-1 and CSR-1 IP (data not shown). The extract without any IP was used to prepare the Input small RNAs. Input and co-IP small RNAs were extracted using Phenol::$CHCl_3$ and sequenced as described in the previous section.

Data availability

Fastq files for the small RNA sequencing results have been deposited in NCBI with the GEO accession number GSE196847.

Bioinformatic analysis

To extract the small RNA reads, we first trimmed the 3'linker sequence from the raw Illumina reads. We added a set of four 4-nt barcodes at the 5' end of small RNAs for each library. We collapsed identical small RNA reads with identical barcodes to minimize bottlenecking caused by 0PCR amplification (identical small RNA reads with different barcodes were not collapsed). All sequence alignments were performed using Bowtie version 1.2.3 (Langmead, Trapnell et al. 2009). The 5' barcodes were trimmed at the step of alignment. Only the 20-24nt sRNA reads that perfectly aligned to the reference sequence were used for the analysis. Custom scripts are available upon requests.

siRNA track plot, index calculation, and statistics

Customized python scripts were used to make the siRNA track plots, in which individual sequenced sRNAs were drawn based on their alignment locations. Sense and antisense siRNAs were plotted separately above and below the gene track, respectively. Only perfectly aligned reads were used for the plots. When SNPs were used in the reference, reads were colored coded as indicated in the figure

legends. Briefly, a red track covers a SNP position and contains the SNP base used in the reference (therefore definitely derided from the SNP-containing reference). A gray track does not cover any SNP position, therefore can be derived from either the SNP-contain reference or the homologous target gene. Reads outside of the inserted sequence are colored in black. Reads covering the junctions of insertions are in orange. In some cases we also made the small RNA coverage plots (in R) by counting the number of sequenced reads at each base position, normalized by the sequencing depth (in millions).

The siRNA suppression index for insertions in *Cer3* was calculated as the ratio between antisense siRNAs density in the 400 nt flanking sequences and the inserted sequence. Note that the ambiguous insertion siRNAs (ones do not cover any SNP position) were included for the calculation. Since some of the ambiguous siRNAs may come from the native gene, the true siRNA suppression index is likely to be higher than the calculated value.

To calculate the statistical significance of the siRNA suppression, we divided the insertion sequence and the 400 bp *Cer3* flanking sequences (left and right) into 50 nt bins. The number of siRNAs matching to each bin were counted. The Wilcoxon Rank Sum Test was performed for these two populations: counts for the insertion bins (G) and counts for the flanking bins (F), with the null hypothesis being G≥F.

Auxin-induced protein degradation (AID) of CSR-1

The degron-3xflag tag was added to the N-terminus of the longer isoform of CSR-1 (F20D12.1a) by CRISPR in the strain that carries the *Cer3::oma-1(red20)* and *sun-1p::TIR1::mRuby::sun-1 3'UTR* (Zhang, Ward et al. 2015). Synchronized L1 larvae were cultured on plates containing 1 mM auxin or no auxin (as control) until reaching young adults, which were harvested for sRNA-seq. CSR-1 AID was confirmed by both western blotting using the monoclonal anti-FLAG M2 antibody (Sigma, F1804-200UG, Lot: SLBG5673V) (Fig. S7) and the sterility of auxin-treated animals (data not shown).

piRNA interference (piRNAi)

oma-1 piRNAi was induced by an extrachromosomal array carrying the hygromycin-resistance gene and a cluster of piRNA expression units re-coded to target *oma-1* as described in (Priyadarshini, Ni et al. 2022). The control *unc-119* piRNAi transgene was also the same as used in (Priyadarshini, Ni et al. 2022). The extrachromosomal array was selected by hygromycin resistance. The *oma-1* insertion used in the *Cer3::oma-1* (*red20*) allele contains two sites that can be targeted by piRNAs from the transgene. To rule out that the effect on siRNA suppression was due to interaction between *oma-1* piRNAs and *Cer3::oma-1*, we created a new *Cer3::oma-1* allele (*red118*) that deleted the two piRNA-target sites.

***oma-1* mRNA expression analysis**

oma-1 mRNA levels were measured by either RT-qPCR or RNA-seq as described(Kalinava, Ni et al. 2017).

Acknowledgement:

We thank Esteban Chen, Natallia Kalinava, Helen Ushakov, and Elaine Gavin for technical assistance. We thank Andrew Fire for providing the python plotting program Very Simply Graphic (VSG). Research reported in this publication was supported by the Busch Biomedical Grant from Rutgers University and the National Institute of General Medical Sciences of the National Institutes of Health under award number R01GM111752 to SG and by KAUST Office of Sponsored Research OSR-CRG2019-4016 to CFJ. Some strains were provided by the CGC, which is funded by NIH Office of Research Infrastructure Programs (P40 OD010440). The content is solely the responsibility of the authors and does not necessarily represent the official views of the funding agencies, including the National Institutes of Health. The authors have no competing interests in this work.

Reference

Alcazar, R. M., R. Lin and A. Z. Fire (2008). "Transmission dynamics of heritable silencing induced by double-stranded RNA in Caenorhabditis elegans." Genetics **180**(3): 1275-1288.

Ameres, S. L., M. D. Horwich, J. H. Hung, J. Xu, M. Ghildiyal, Z. Weng and P. D. Zamore (2010). "Target RNA-directed trimming and tailing of small silencing RNAs." Science **328**(5985): 1534-1539.

Arribere, J. A., R. T. Bell, B. X. Fu, K. L. Artiles, P. S. Hartman and A. Z. Fire (2014). "Efficient marker-free recovery of custom genetic modifications with CRISPR/Cas9 in Caenorhabditis elegans." Genetics **198**(3): 837-846.

Ashe, A., A. Sapetschnig, E. M. Weick, J. Mitchell, M. P. Bagijn, A. C. Cording, A. L. Doebley, L. D. Goldstein, N. J. Lehrbach, J. Le Pen, G. Pintacuda, A. Sakaguchi, P. Sarkies, S. Ahmed and E. A. Miska (2012). "piRNAs can trigger a multigenerational epigenetic memory in the germline of C. elegans." Cell **150**(1): 88-99.

Batista, P. J., J. G. Ruby, J. M. Claycomb, R. Chiang, N. Fahlgren, K. D. Kasschau, D. A. Chaves, W. Gu, J. J. Vasale, S. Duan, D. Conte, Jr., S. Luo, G. P. Schroth, J. C. Carrington, D. P. Bartel and C. C. Mello (2008). "PRG-1 and 21U-RNAs interact to form the piRNA complex required for fertility in C. elegans." Mol Cell **31**(1): 67-78.

Beltran, T., V. Shahrezaei, V. Katju and P. Sarkies (2020). "Epimutations driven by small RNAs arise frequently but most have limited duration in Caenorhabditis elegans." Nat Ecol Evol **4**(11): 1539-1548.

Billi, A. C., S. E. Fischer and J. K. Kim (2014). "Endogenous RNAi pathways in C. elegans." WormBook: 1-49.

Brenner, S. (1974). "The genetics of Caenorhabditis elegans." Genetics **77**(1): 71-94.

Buckley, B. A., K. B. Burkhart, S. G. Gu, G. Spracklin, A. Kershner, H. Fritz, J. Kimble, A. Fire and S. Kennedy (2012). "A nuclear Argonaute promotes multigenerational epigenetic inheritance and germline immortality." Nature **489**(7416): 447-451.

Campbell, A. C. and D. L. Updike (2015). "CSR-1 and P granules suppress sperm-specific transcription in the C. elegans germline." Development **142**(10): 1745-1755.

Cecere, G., S. Hoersch, S. O'Keeffe, R. Sachidanandam and A. Grishok (2014). "Global effects of the CSR-1 RNA interference pathway on the transcriptional landscape." Nat Struct Mol Biol **21**(4): 358-365.

Charlesworth, A. G., U. Seroussi, N. J. Lehrbach, M. S. Renaud, A. E. Sundby, R. I. Molnar, R. X. Lao, A. R. Willis, J. R. Woock, M. J. Aber, A. J. Diao, A. W. Reinke, G. Ruvkun and J. M. Claycomb (2021). "Two isoforms of the essential C. elegans Argonaute CSR-1 differentially regulate sperm and oocyte fertility." Nucleic Acids Res **49**(15): 8836-8865.

Claycomb, J. M., P. J. Batista, K. M. Pang, W. Gu, J. J. Vasale, J. C. van Wolfswinkel, D. A. Chaves, M. Shirayama, S. Mitani, R. F. Ketting, D. Conte, Jr. and C. C. Mello (2009). "The Argonaute CSR-1 and its 22G-RNA cofactors are required for holocentric chromosome segregation." Cell **139**(1): 123-134.
Consortium, C. e. D. M. (2012). "large-scale screening for targeted knockouts in the Caenorhabditis elegans genome." G3 (Bethesda) **2**(11): 1415-1425.
de Albuquerque, B. F., M. Placentino and R. F. Ketting (2015). "Maternal piRNAs Are Essential for Germline Development following De Novo Establishment of Endo-siRNAs in Caenorhabditis elegans." Dev Cell **34**(4): 448-456.
Devanapally, S., P. Raman, M. Chey, S. Allgood, F. Ettefa, M. Diop, Y. Lin, Y. E. Cho and A. M. Jose (2021). "Mating can initiate stable RNA silencing that overcomes epigenetic recovery." Nat Commun **12**(1): 4239.
Dokshin, G. A., K. S. Ghanta, K. M. Piscopo and C. C. Mello (2018). "Robust Genome Editing with Short Single-Stranded and Long, Partially Single-Stranded DNA Donors in Caenorhabditis elegans." Genetics **210**(3): 781-787.
Fassnacht, C., C. Tocchini, P. Kumari, D. Gaidatzis, M. B. Stadler and R. Ciosk (2018). "The CSR-1 endogenous RNAi pathway ensures accurate transcriptional reprogramming during the oocyte-to-embryo transition in Caenorhabditis elegans." PLoS Genet **14**(3): e1007252.
Fire, A., S. Xu, M. K. Montgomery, S. A. Kostas, S. E. Driver and C. C. Mello (1998). "Potent and specific genetic interference by double-stranded RNA in Caenorhabditis elegans." Nature **391**(6669): 806-811.
Gent, J. I., A. T. Lamm, D. M. Pavelec, J. M. Maniar, P. Parameswaran, L. Tao, S. Kennedy and A. Z. Fire (2010). "Distinct phases of siRNA synthesis in an endogenous RNAi pathway in C. elegans soma." Mol Cell **37**(5): 679-689.
Gerson-Gurwitz, A., S. Wang, S. Sathe, R. Green, G. W. Yeo, K. Oegema and A. Desai (2016). "A Small RNA-Catalytic Argonaute Pathway Tunes Germline Transcript Levels to Ensure Embryonic Divisions." Cell **165**(2): 396-409.
Gloeckner, C. J., K. Boldt and M. Ueffing (2009). "Strep/FLAG tandem affinity purification (SF-TAP) to study protein interactions." Curr Protoc Protein Sci **Chapter 19**: Unit19 20.
Grishok, A., H. Tabara and C. C. Mello (2000). "Genetic requirements for inheritance of RNAi in C. elegans." Science **287**(5462): 2494-2497.
Gu, W., M. Shirayama, D. Conte, Jr., J. Vasale, P. J. Batista, J. M. Claycomb, J. J. Moresco, E. M. Youngman, J. Keys, M. J. Stoltz, C. C. Chen, D. A. Chaves, S. Duan, K. D. Kasschau, N. Fahlgren, J. R. Yates, 3rd, S. Mitani, J. C. Carrington and C. C. Mello (2009). "Distinct argonaute-mediated 22G-RNA pathways direct genome surveillance in the C. elegans germline." Mol Cell **36**(2): 231-244.
Guang, S., A. F. Bochner, K. B. Burkhart, N. Burton, D. M. Pavelec and S. Kennedy (2010). "Small regulatory RNAs inhibit RNA polymerase II during the elongation phase of transcription." Nature **465**(7301): 1097-1101.
Gudipati, R. K., K. Braun, F. Gypas, D. Hess, J. Schreier, S. H. Carl, R. F. Ketting and H. Grosshans (2021). "Protease-mediated processing of Argonaute proteins controls small RNA association." Mol Cell **81**(11): 2388-2402 e2388.
Han, T., A. P. Manoharan, T. T. Harkins, P. Bouffard, C. Fitzpatrick, D. S. Chu, D. Thierry-Mieg, J. Thierry-Mieg and J. K. Kim (2009). "26G endo-siRNAs regulate spermatogenic and zygotic gene expression in Caenorhabditis elegans." Proc Natl Acad Sci U S A **106**(44): 18674-18679.
Johnson, C. L. and A. M. Spence (2011). "Epigenetic licensing of germline gene expression by maternal RNA in C. elegans." Science **333**(6047): 1311-1314.
Kalinava, N., J. Z. Ni, K. Peterman, E. Chen and S. G. Gu (2017). "Decoupling the downstream effects of germline nuclear RNAi reveals that H3K9me3 is dispensable for heritable RNAi and the maintenance of endogenous siRNA-mediated transcriptional silencing in Caenorhabditis elegans." Epigenetics Chromatin **10**: 6.

Kasper, D. M., G. Wang, K. E. Gardner, T. G. Johnstone and V. Reinke (2014). "The C. elegans SNAPc component SNPC-4 coats piRNA domains and is globally required for piRNA abundance." Dev Cell **31**(2): 145-158.
Langmead, B., C. Trapnell, M. Pop and S. L. Salzberg (2009). "Ultrafast and memory-efficient alignment of short DNA sequences to the human genome." Genome Biol **10**(3): R25.
Lee, H. C., W. Gu, M. Shirayama, E. Youngman, D. Conte, Jr. and C. C. Mello (2012). "C. elegans piRNAs mediate the genome-wide surveillance of germline transcripts." Cell **150**(1): 78-87.
Makeyeva, Y. V., M. Shirayama and C. C. Mello (2021). "Cues from mRNA splicing prevent default Argonaute silencing in C. elegans." Dev Cell **56**(18): 2636-2648 e2634.
Maniar, J. M. and A. Z. Fire (2011). "EGO-1, a C. elegans RdRP, modulates gene expression via production of mRNA-templated short antisense RNAs." Curr Biol **21**(6): 449-459.
Marnik, E. A. and D. L. Updike (2019). "Membraneless organelles: P granules in Caenorhabditis elegans." Traffic **20**(6): 373-379.
Montgomery, B. E., T. Vijayasarathy, T. N. Marks, C. A. Cialek, K. J. Reed and T. A. Montgomery (2021). "Dual roles for piRNAs in promoting and preventing gene silencing in C. elegans." Cell Rep **37**(10): 110101.
Newman, M. A., F. Ji, S. E. J. Fischer, A. Anselmo, R. I. Sadreyev and G. Ruvkun (2018). "The surveillance of pre-mRNA splicing is an early step in C. elegans RNAi of endogenous genes." Genes Dev **32**(9-10): 670-681.
Ni, J. Z., E. Chen and S. G. Gu (2014). "Complex coding of endogenous siRNA, transcriptional silencing and H3K9 methylation on native targets of germline nuclear RNAi in C. elegans." BMC Genomics **15**: 1157.
Ni, J. Z., N. Kalinava, E. Chen, A. Huang, T. Trinh and S. G. Gu (2016). "A transgenerational role of the germline nuclear RNAi pathway in repressing heat stress-induced transcriptional activation in C. elegans." Epigenetics Chromatin **9**: 3.
Ni, J. Z., N. Kalinava, S. G. Mendoza and S. G. Gu (2018). "The spatial and temporal dynamics of nuclear RNAi-targeted retrotransposon transcripts in Caenorhabditis elegans." Development.
Paix, A., A. Folkmann, D. Rasoloson and G. Seydoux (2015). "High Efficiency, Homology-Directed Genome Editing in Caenorhabditis elegans Using CRISPR-Cas9 Ribonucleoprotein Complexes." Genetics **201**(1): 47-54.
Phillips, C. M., K. C. Brown, B. E. Montgomery, G. Ruvkun and T. A. Montgomery (2015). "piRNAs and piRNA-Dependent siRNAs Protect Conserved and Essential C. elegans Genes from Misrouting into the RNAi Pathway." Dev Cell **34**(4): 457-465.
Piatek, M. J. and A. Werner (2014). "Endogenous siRNAs: regulators of internal affairs." Biochem Soc Trans **42**(4): 1174-1179.
Pisacane, P. and M. Halic (2017). "Tailing and degradation of Argonaute-bound small RNAs protect the genome from uncontrolled RNAi." Nat Commun **8**: 15332.
Priyadarshini, M., J. Z. Ni, A. M. Vargas-Velazquez, S. G. Gu and C. Frokjaer-Jensen (2022). "Reprogramming the piRNA pathway for multiplexed and transgenerational gene silencing in C. elegans." Nat Methods **19**(2): 187-194.
Reed, K. J., J. M. Svendsen, K. C. Brown, B. E. Montgomery, T. N. Marks, T. Vijayasarathy, D. M. Parker, E. O. Nishimura, D. L. Updike and T. A. Montgomery (2020). "Widespread roles for piRNAs and WAGO-class siRNAs in shaping the germline transcriptome of Caenorhabditis elegans." Nucleic Acids Res **48**(4): 1811-1827.
Serizay, J., Y. Dong, J. Janes, M. Chesney, C. Cerrato and J. Ahringer (2020). "Distinctive regulatory architectures of germline-active and somatic genes in C. elegans." Genome Res **30**(12): 1752-1765.

Seth, M., M. Shirayama, W. Gu, T. Ishidate, D. Conte, Jr. and C. C. Mello (2013). "The C. elegans CSR-1 argonaute pathway counteracts epigenetic silencing to promote germline gene expression." Dev Cell **27**(6): 656-663.
Seth, M., M. Shirayama, W. Tang, E. Z. Shen, S. Tu, H. C. Lee, Z. Weng and C. C. Mello (2018). "The Coding Regions of Germline mRNAs Confer Sensitivity to Argonaute Regulation in C. elegans." Cell Rep **22**(9): 2254-2264.
Seydoux, G. (2018). "The P Granules of C. elegans: A Genetic Model for the Study of RNA-Protein Condensates." J Mol Biol **430**(23): 4702-4710.
Shen, E. Z., H. Chen, A. R. Ozturk, S. Tu, M. Shirayama, W. Tang, Y. H. Ding, S. Y. Dai, Z. Weng and C. C. Mello (2018). "Identification of piRNA Binding Sites Reveals the Argonaute Regulatory Landscape of the C. elegans Germline." Cell **172**(5): 937-951 e918.
Sheu-Gruttadauria, J., P. Pawlica, S. M. Klum, S. Wang, T. A. Yario, N. T. Schirle Oakdale, J. A. Steitz and I. J. MacRae (2019). "Structural Basis for Target-Directed MicroRNA Degradation." Mol Cell **75**(6): 1243-1255 e1247.
Shirayama, M., M. Seth, H. C. Lee, W. Gu, T. Ishidate, D. Conte, Jr. and C. C. Mello (2012). "piRNAs initiate an epigenetic memory of nonself RNA in the C. elegans germline." Cell **150**(1): 65-77.
Shukla, A., J. Yan, D. J. Pagano, A. E. Dodson, Y. Fei, J. Gorham, J. G. Seidman, M. Wickens and S. Kennedy (2020). "poly(UG)-tailed RNAs in genome protection and epigenetic inheritance." Nature **582**(7811): 283-288.
Strome, S. and W. B. Wood (1982). "Immunofluorescence visualization of germ-line-specific cytoplasmic granules in embryos, larvae, and adults of Caenorhabditis elegans." Proc Natl Acad Sci U S A **79**(5): 1558-1562.
van Wolfswinkel, J. C., J. M. Claycomb, P. J. Batista, C. C. Mello, E. Berezikov and R. F. Ketting (2009). "CDE-1 affects chromosome segregation through uridylation of CSR-1-bound siRNAs." Cell **139**(1): 135-148.
Vastenhouw, N. L., K. Brunschwig, K. L. Okihara, F. Muller, M. Tijsterman and R. H. Plasterk (2006). "Gene expression: long-term gene silencing by RNAi." Nature **442**(7105): 882.
Wahba, L., L. Hansen and A. Z. Fire (2021). "An essential role for the piRNA pathway in regulating the ribosomal RNA pool in C. elegans." Dev Cell **56**(16): 2295-2312 e2296.
Wang, Y., C. Weng, X. Chen, X. Zhou, X. Huang, Y. Yan and C. Zhu (2020). "CDE-1 suppresses the production of risiRNA by coupling polyuridylation and degradation of rRNA." BMC Biol **18**(1): 115.
Weick, E. M., P. Sarkies, N. Silva, R. A. Chen, S. M. Moss, A. C. Cording, J. Ahringer, E. Martinez-Perez and E. A. Miska (2014). "PRDE-1 is a nuclear factor essential for the biogenesis of Ruby motif-dependent piRNAs in C. elegans." Genes Dev **28**(7): 783-796.
Yang, A., T. J. Shao, X. Bofill-De Ros, C. Lian, P. Villanueva, L. Dai and S. Gu (2020). "AGO-bound mature miRNAs are oligouridylated by TUTs and subsequently degraded by DIS3L2." Nat Commun **11**(1): 2765.
Zhang, L., J. D. Ward, Z. Cheng and A. F. Dernburg (2015). "The auxin-inducible degradation (AID) system enables versatile conditional protein depletion in C. elegans." Development **142**(24): 4374-4384.
Zhou, X., X. Feng, H. Mao, M. Li, F. Xu, K. Hu and S. Guang (2017). "RdRP-synthesized antisense ribosomal siRNAs silence pre-rRNA via the nuclear RNAi pathway." Nat Struct Mol Biol **24**(3): 258-269.

Figures

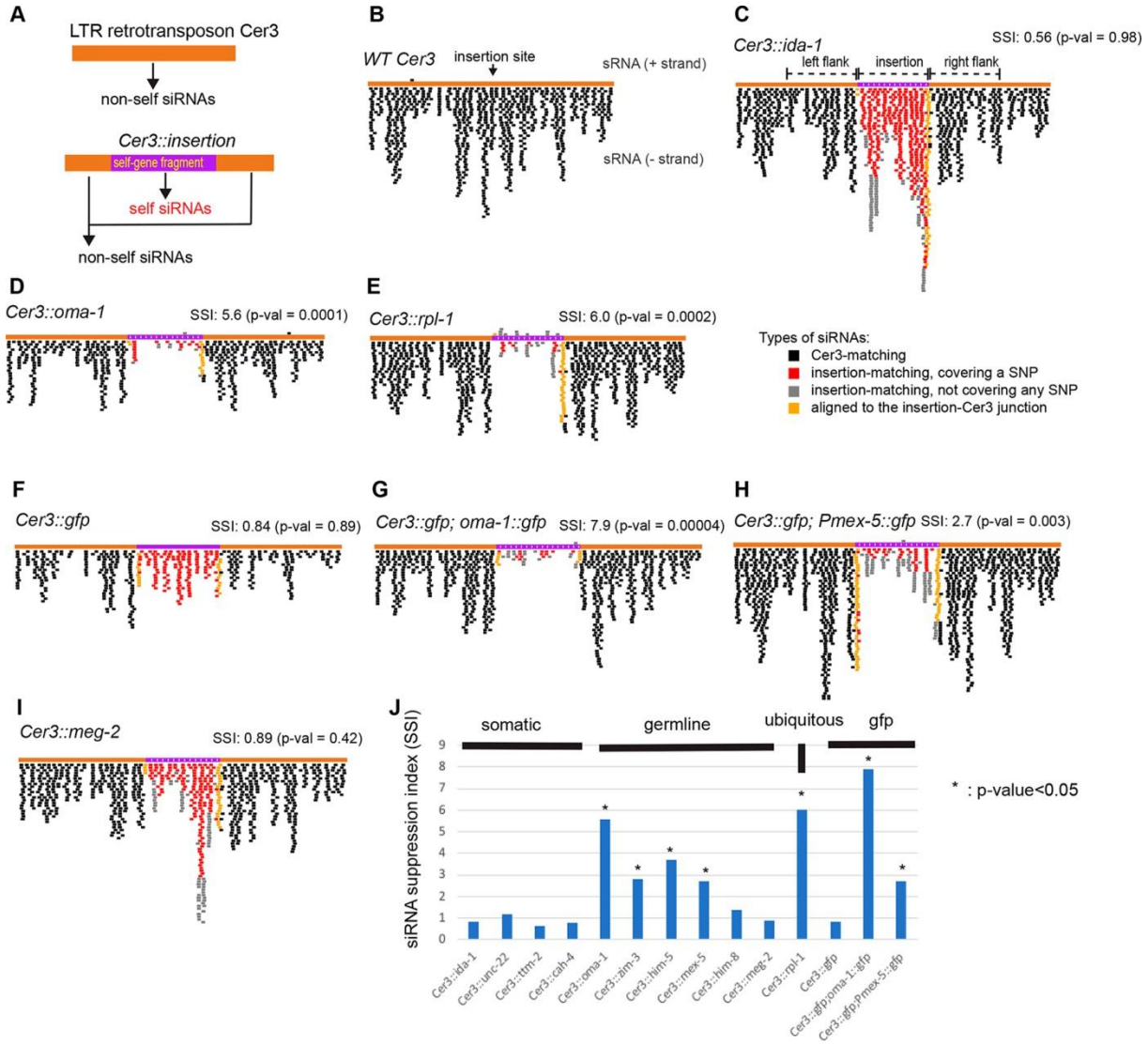

Fig. 1. Differential expression of ectopic self siRNAs driven by LTR retrotransposon *Cer3*. (**A**) A schematic diagram of *Cer3* with a CRISPR-engineered insertion (*Cer3::insertion*) to express ectopic siRNAs. (**B**-**I**) siRNA track plots for WT *Cer3* and various *Cer3::insertion* alleles. Only the insertion and the 1.4 kb *Cer3* sequence (700 bp on either side of the insertion) are included in the plots. Individual sense and antisense small RNA reads with perfect alignment to the *Cer3::insertion* sequences are plotted above and below the gene track, respectively. siRNA tracks are color-coded to reflect their locations as indicated in the legend. Additional *Cer3::insertion* siRNA track plots are in Fig. S4. The *s*iRNA *s*uppression *i*ndex (SSI=*Cer3* siRNA density of the 400 bp left and right flanking sequences / siRNA density of the insertion) and p-value are indicated for each panel. (**J**) A bar graph of siRNA suppression indexes for various *Cer3* alleles shown in Fig. 1 and S4. The p-values were calculated by using Wilcoxon Rank Sum Test with the null hypothesis that the density of siRNAs mapped to the insertion is the same or larger than the density of flanking *Cer3* siRNAs.

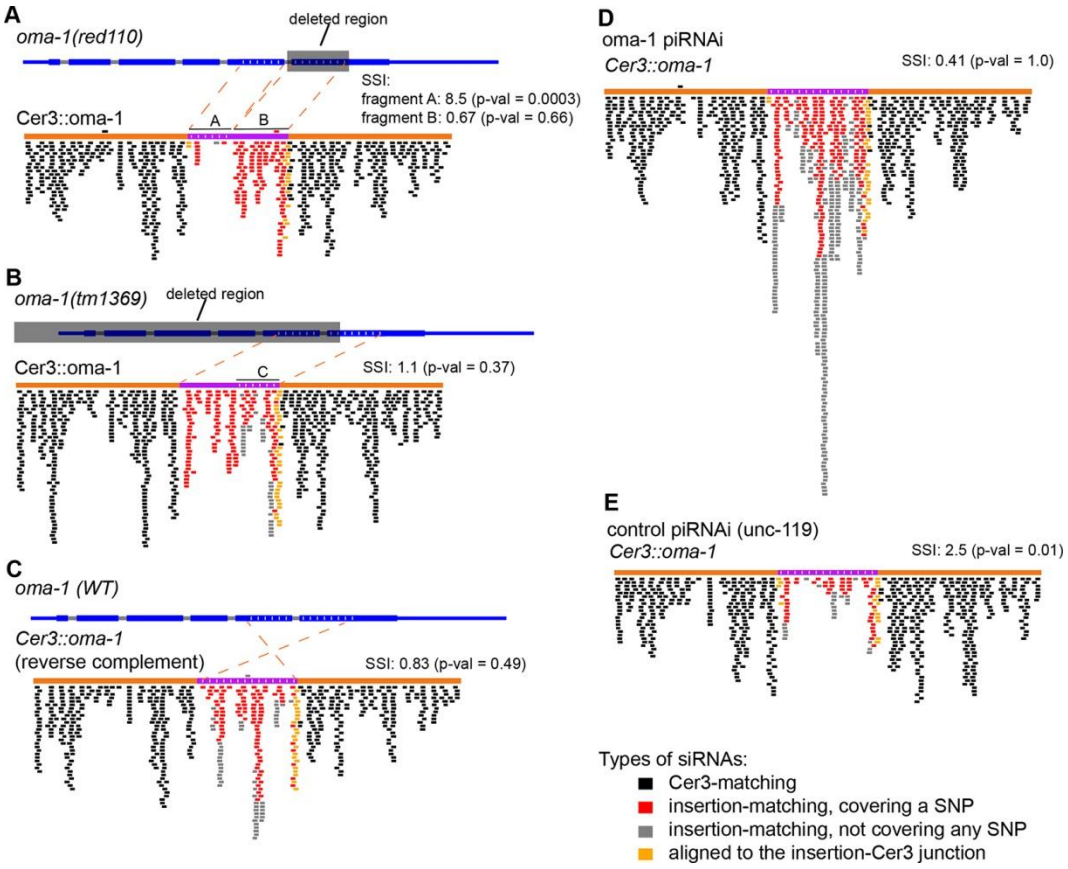

Fig. 2. siRNA suppression requires the mRNA expression of the homologous gene. (**A**-**B**) *Cer3::oma-1* siRNA track plots for strains carrying *oma-1* deletion mutations (A: *red110,* B: *tm1396*). Deleted regions are indicated by transparent grey boxes. (**C**) A siRNA track plot for *Cer3::oma-1* that expresses sense-stranded *oma-1* siRNAs. (**D**-**E**) siRNA track plots for *Cer3::oma-1* in *oma-1* piRNAi animals and in control animals (*unc-119* piRNAi). See Fig. S5 for mRNA-seq results of piRNAi-induced *oma-1* mRNA silencing and Fig. S6 for additional experiments of *oma-1* piRNAi.

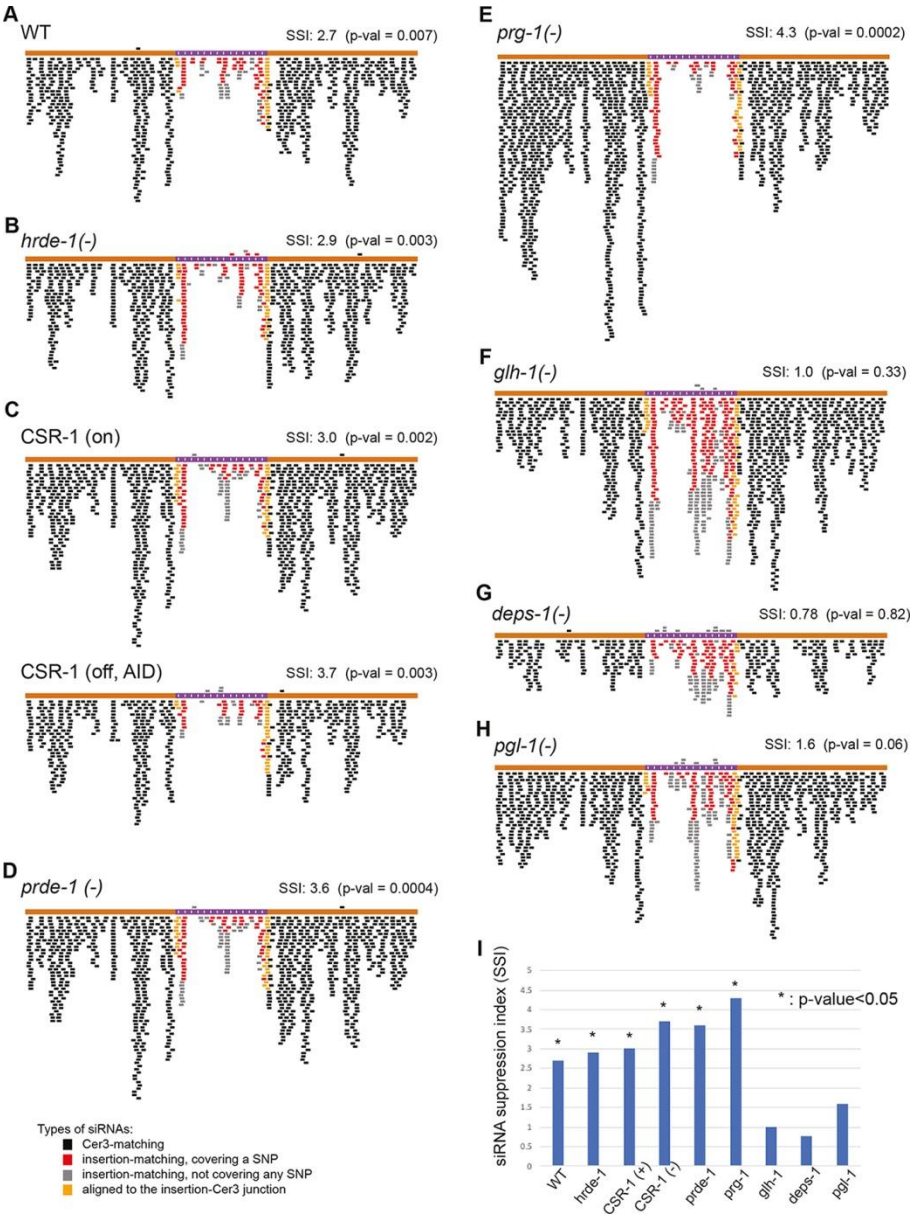

Fig. 3. Genetic requirement of siRNA suppression of *Cer3::oma-1.* (**A-B**, **D**-**H**): *Cer3::oma-1* siRNA track plots for wild type animals and various loss-of-function mutants as indicated in each panel. (**C**) *Cer3::oma-1* siRNA track plots for animals with auxin-induced degradation (AID) of CSR-1 (lower panel) and control animals (upper panel). See Fig. S7 for the CSR-1 western blotting result. (**I**) A bar graph of siRNA suppression indexes (SSIs) for the experiments shown in panels A-H.

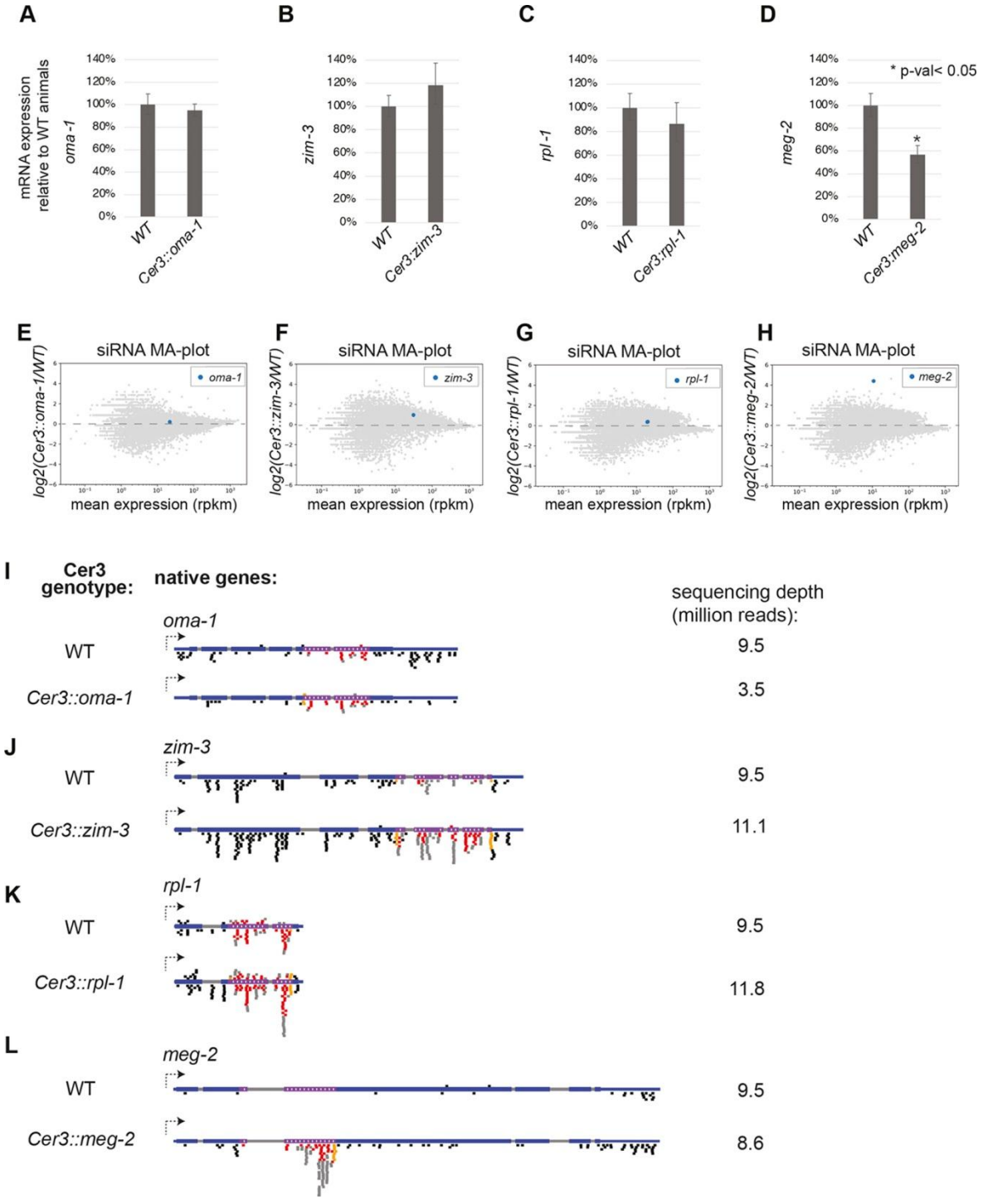

Fig. 4. The impact of *Cer3*-driven ectopic siRNAs on target gene mRNA and siRNA expressions. (**A**-**D**) RT-qPCR analysis of the corresponding target gene mRNA for WT and *Cer3* mutant animals. (**E**-**H**) sRNA-seq analysis (MA [log-ratio vs mean average]-plots) comparing WT and a *Cer3* mutant strain for all genes. The corresponding target gene in each panel is highlighted. (**I**-**L**) sRNA track plots for corresponding target genes of the ectopic siRNAs expressed from the *Cer3::insertion* alleles (the bottom plot in each

panel). The top plot in each panel shows the sRNA profile of the same gene in WT *Cer3* animals. The region homologous to the *Cer3::insertion* was colored in purple with SNPs indicated in vertical lines. SNP matching reads are in red. Reads that are in between two adjacent SNPs are in gray. Reads covering the junctions of the homologous sequence and the flanking sequence are in orange. Arrows indicate the gene transcription direction.

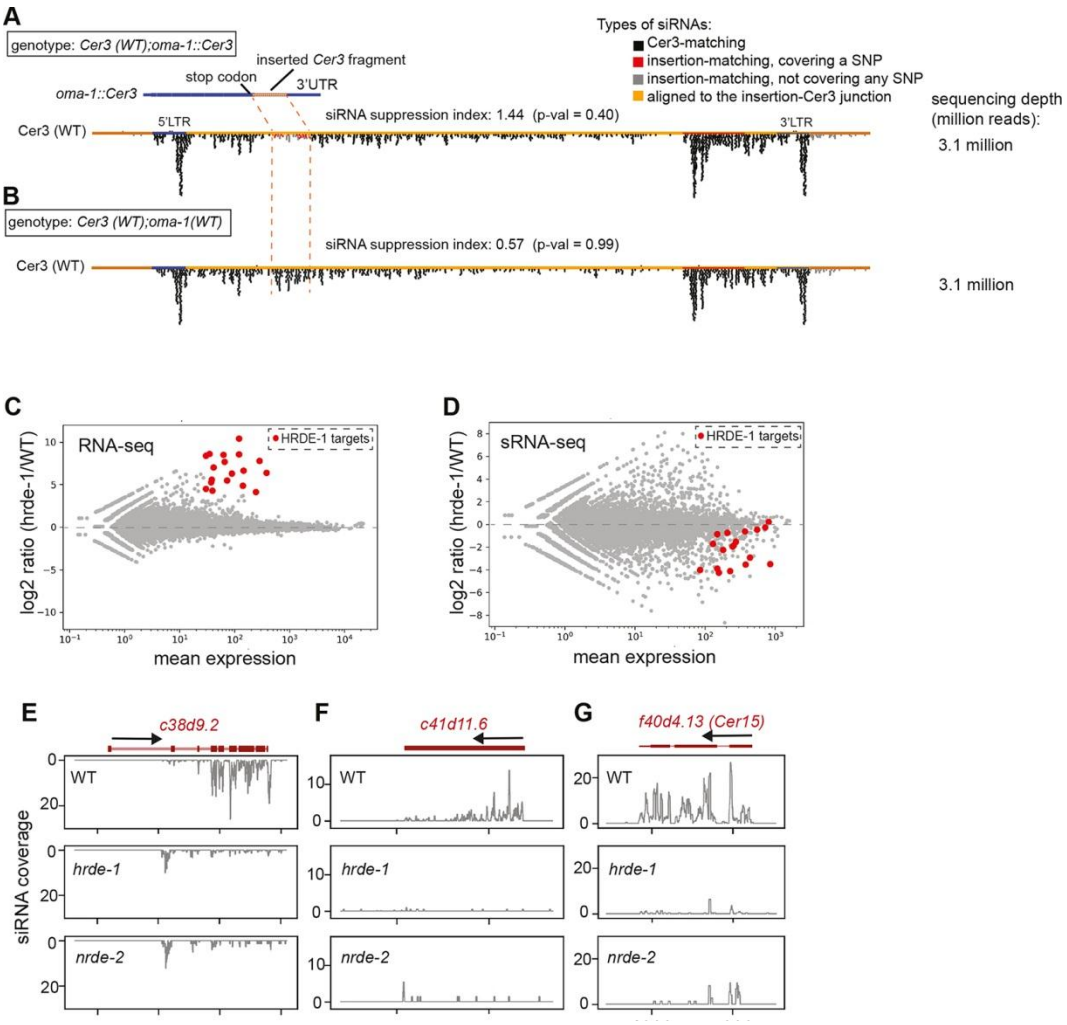

Fig. 5. Suppression of native nonself siRNAs. (**A**) siRNA track plot of a full length WT *Cer3* in the *oma-1::Cer3* mutant, in which a 467 nt *Cer3* sequence was inserted immediately after the stop codon of *oma-1*, with SNPs every 30 nt. (**B**) *Cer3* siRNA track plot for WT animals. The same number of total small RNA reads were used for (A) and (B). A normalized *Cer3* siRNA coverage plot of the same libraries used in (A) and (B) was shown in Fig. S9D. (**C**-**D**) MA (log2 ratio versus mean average)-plots comparing *hrde-1* and WT RNA-seq (C) and sRNA-seq (D). Top 20 HRDE-1 target genes were highlighted in red. (**E**-**G**) sRNA coverage plots for three different HRDE-1 targets in WT, *hrde-1*, and *nrde-2* mutants, as indicated.

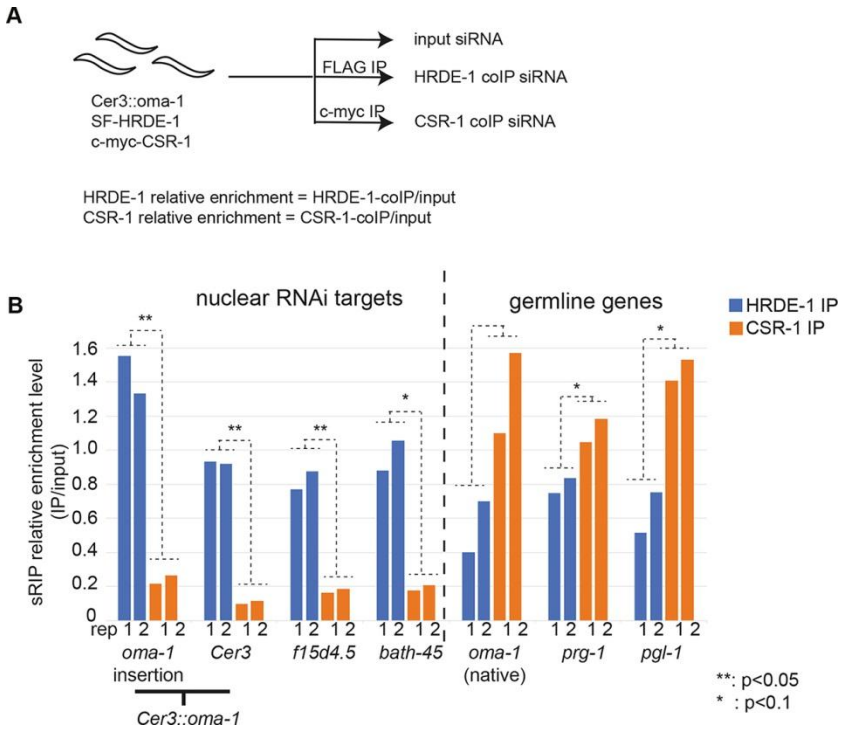

Fig. 6. (**A**) Schematic of the HRDE-1 and CSR-1 (small RNA co-IP) sRIP-seq experiment. (**B**) HRDE-1 and CSR-1 sRIP relative enrichment levels for various genes. Two biological replicates were individually plotted. For *oma-1* insertion of *Cer3::oma-1* , only SNP-containing reads were considered. For *Cer3,* only the 400 nt flanking region on each side of the *oma-1* insertion was used. For the native *oma-1* gene, the *Cer3::oma-1* homologous sequence was excluded from the analysis because *Cer3::oma-1* caused a moderate increase in siRNA levels at this region (data not shown). The full-length cDNA sequences were used for other genes in this panel. A two-tailed Student's t-test was used to calculate the p-values in R.

Fig. 7. A model of the complex interactions between mRNAs and siRNAs: (1) mRNAs are the target of the siRNAs for RNAi, (2) mRNAs are needed for siRNA biogenesis, and (3) mRNAs can also suppress the siRNA production. Nonself genes are active in siRNA biogenesis and RNAi, and inactive in siRNA suppression likely due to the low level of mRNAs. Self genes are active in siRNA suppression likely due to the high level of mRNAs, which at least partially prevents self genes from run-away siRNA amplification and aberrant RNAi activity.

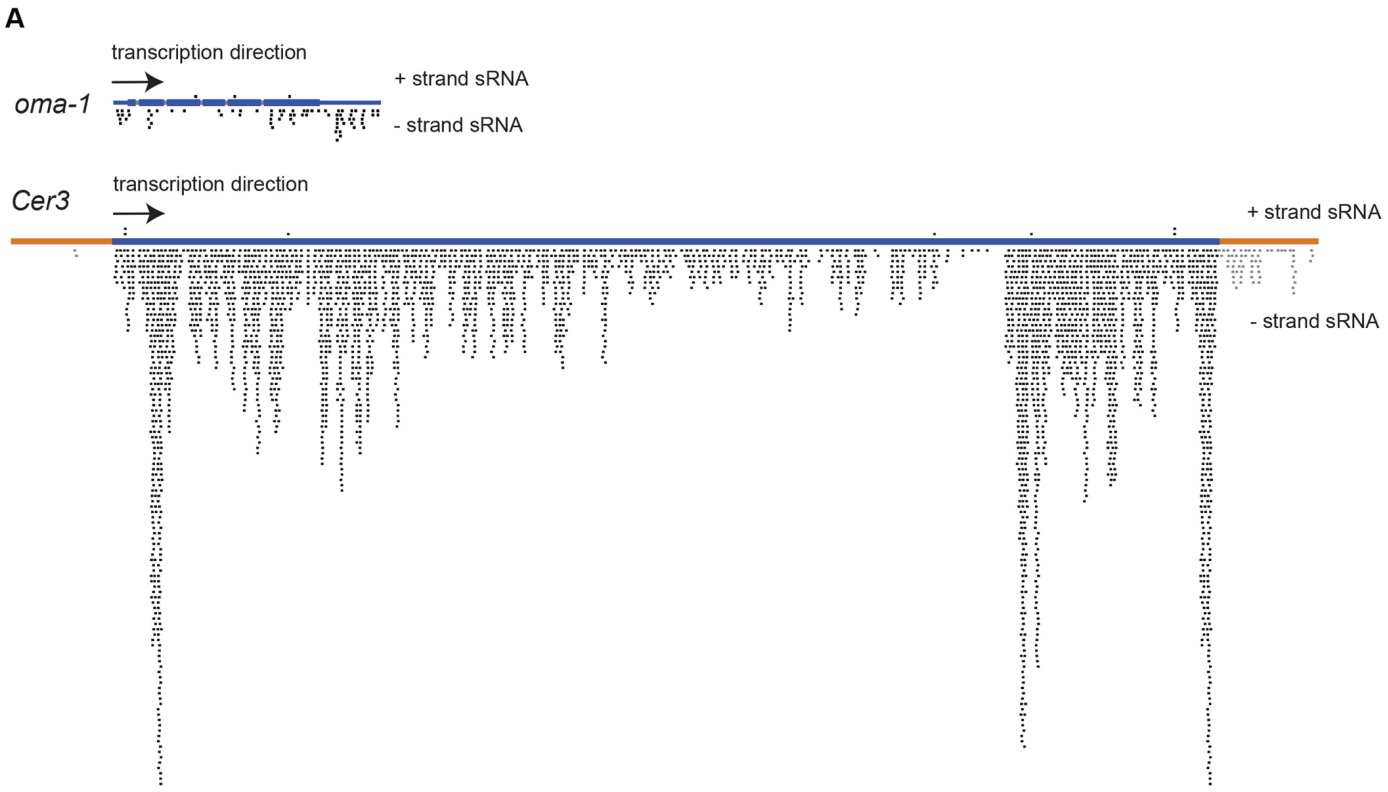

Fig. S1. Differential expression of self and non-self siRNAs. (**A**) siRNA track plots for *oma-1* and the LTR retrotransposon *Cer3* in WT adult animals from the same sequencing run. Each sequenced small RNA read is indicated as a black block above (sense sRNA) or under (antisense sRNA) the gene track. (**B**) Box plot of average siRNA levels of native germline nuclear RNAi targets (non-self siRNAs) and germline genes (self siRNAs) in WT animals. The native germline nuclear RNAi target genes were obtained from (Ni, Chen et al. 2014). The germline genes are the oogenic genes identified in (Ortiz, Noble et al. 2014).

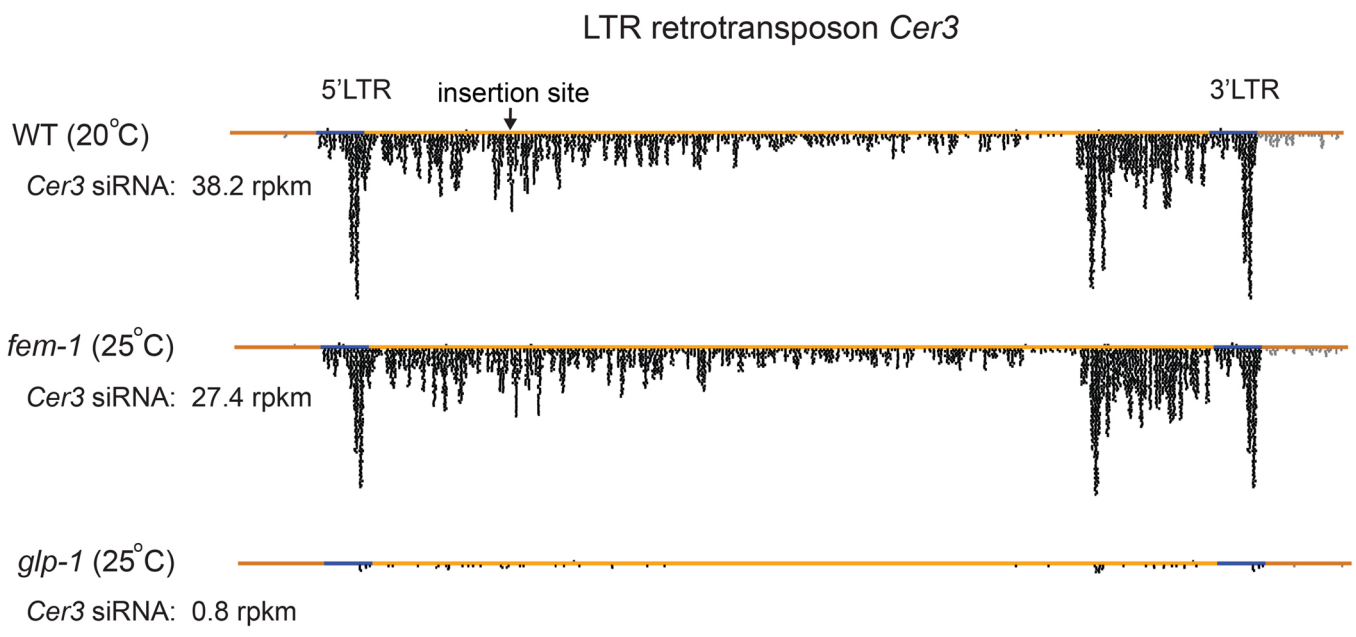

Fig. S2. Germline-enriched expression of *Cer3* siRNAs. *Cer3* siRNA track plots for adult WT (20°C), *fem-1*(*hc17*) (25° C, producing functional female germline, but lack of embryo in the uterus due to spermatogenesis defect) (Nelson, Lew et al. 1978), and *glp-1*(*e2141)* (25°C, germline depleted) (Kodoyianni, Maine et al. 1992) animals. As a quality control for the sRNA-seq, 30%, 12.7%, and 37% of sequenced small RNAs were mapped to microRNAs for WT, *fem-1*, and *glp-1*, respectively. The rpkm values of *Cer3* siRNAs are indicated in the figure. The insertion site in *Cer3* used in this study to express ectopic siRNAs is indicated.

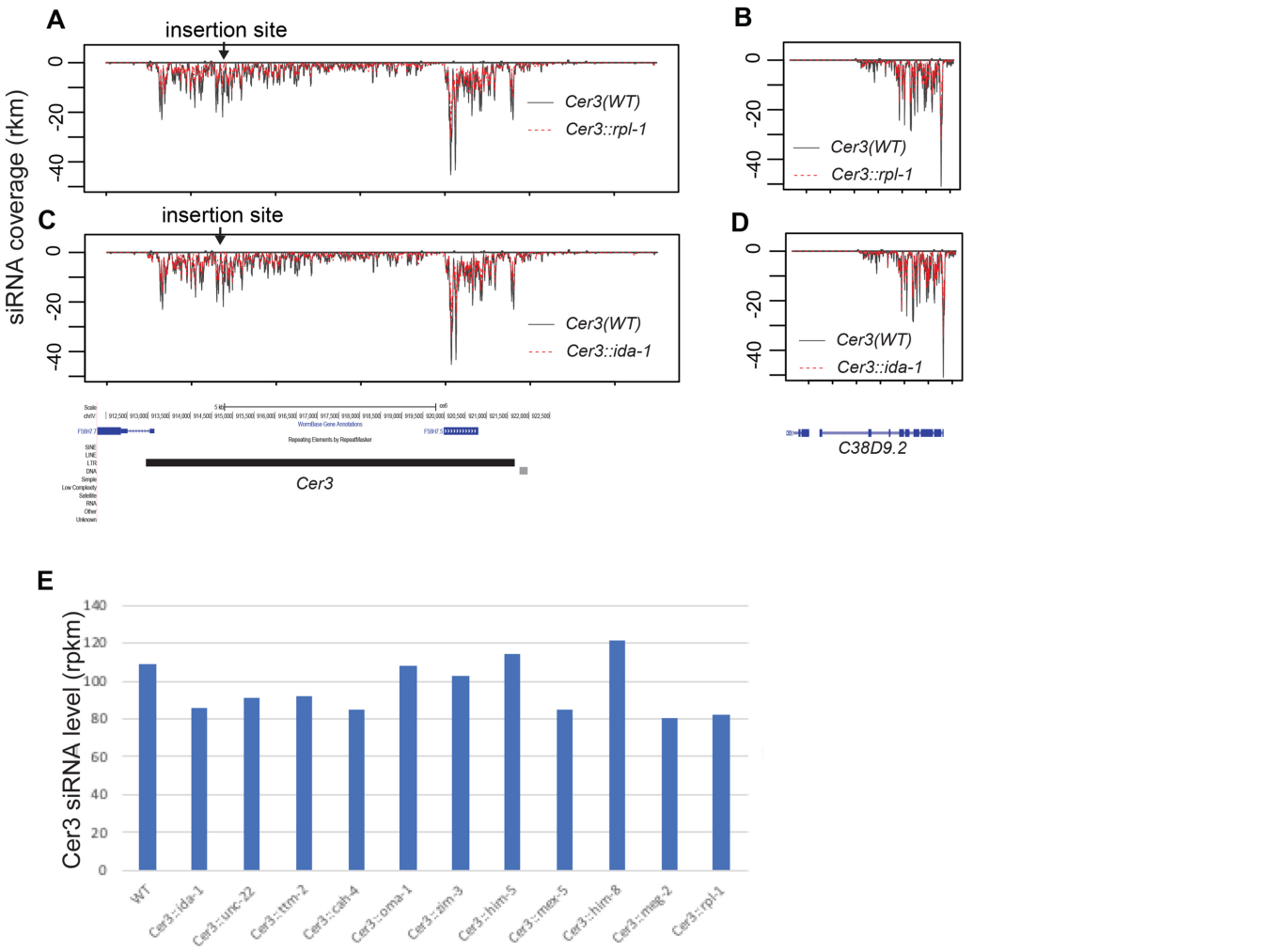

Fig. S3. *Cer3* siRNA expression is not affected by insertions. siRNA coverage plots at *Cer3* (**A** and **C**) and *c38d9.2* (**B** and **D**) are shown for strains carrying WT *Cer3*, *Cer3::rpl-1*, and *Cer3::ida-1* as indicated. Sense and antisense siRNA coverages are separately plotted as positive and negative values. siRNAs derived from the insertion were excluded from this analysis. The WT animals had slightly higher siRNA expressions than the two *Cer3* mutants for *Cer3* and other native nuclear RNAi targets, such as *c38d9.2* (**B** and **D**). This is likely due to a slight age difference between the samples (data not shown). (**E**) Bar graph showing Cer3 siRNA levels (rpkm) for WT and various *Cer3::insertion* mutant stains.

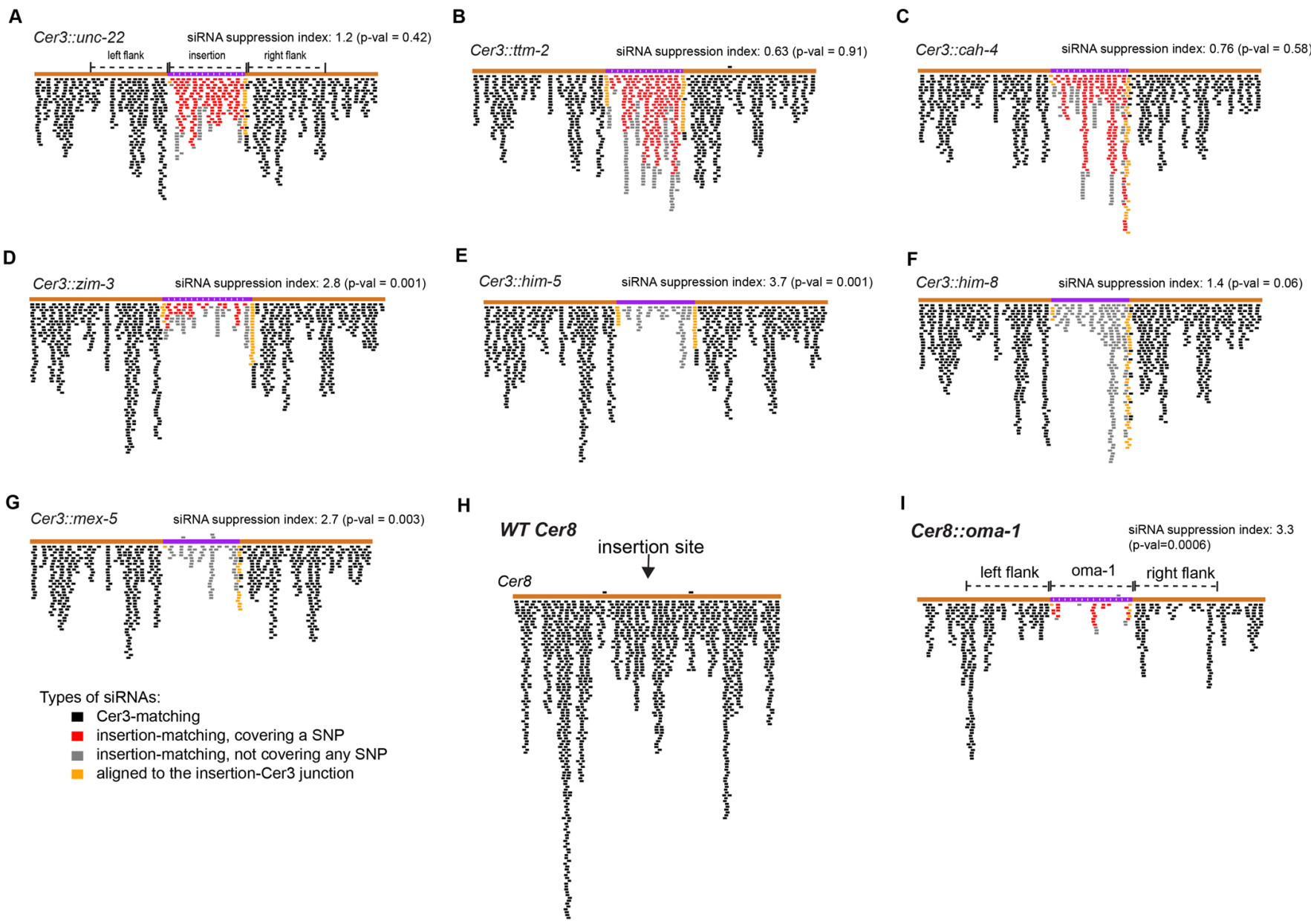

Fig. S4. siRNA track plots of additional *Cer3*::insertions (**A**-**G**), WT LTR retrotransposon *Cer8* (**H**), and *Cer8::oma-1* (**I**). Only the 700 nt *Cer8* sequence that flank each side of the insertion site is used for the plots. For *Cer3::him-5* (E), *Cer3::him-8* (F), and *Cer3::mex-5* (G), no SNPs were included in the insertion and therefore the insertion-matching siRNA reads were all colored in gray.

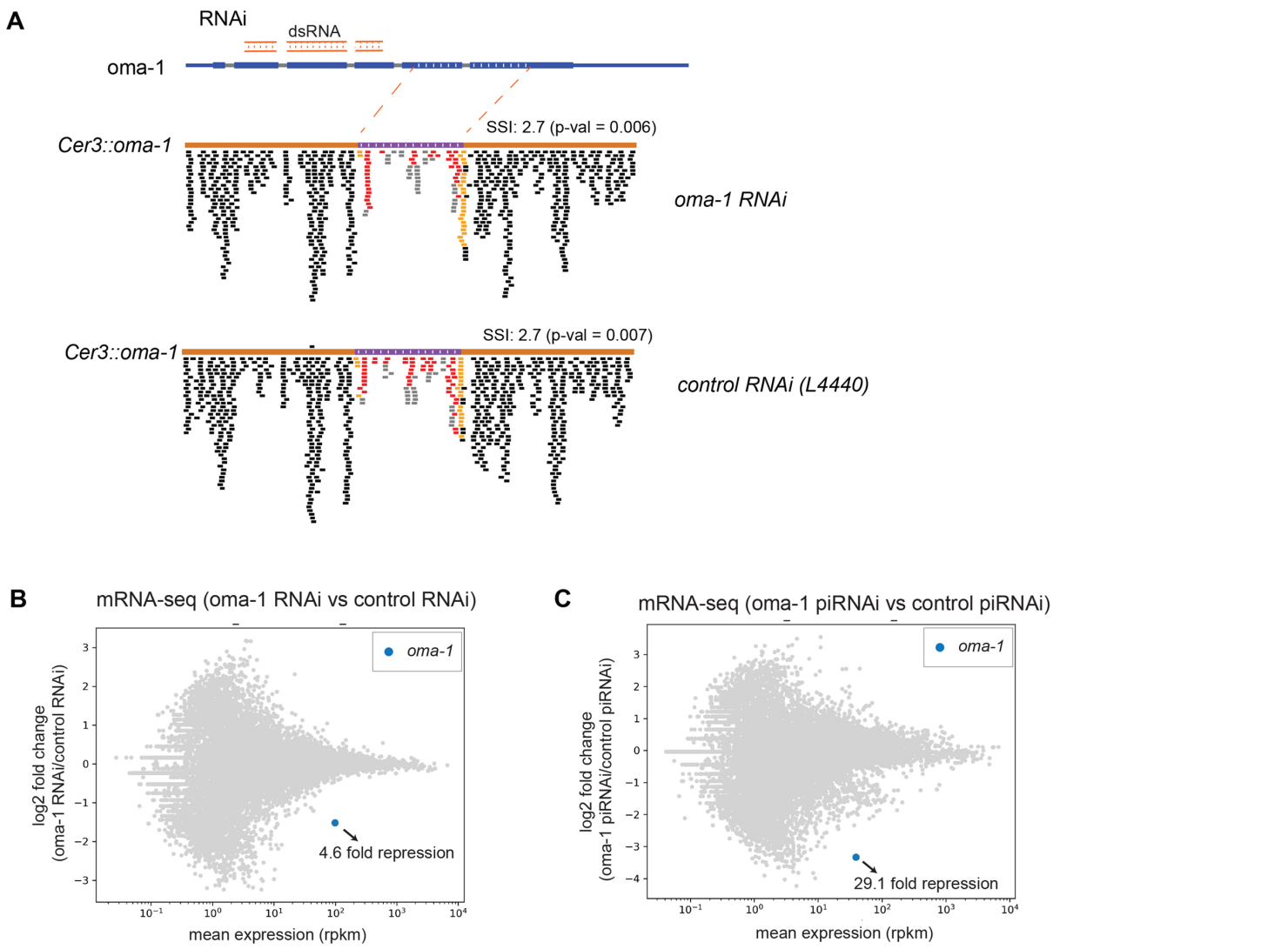

Fig. S5. *oma-1* RNAi did not affect siRNA suppression of *Cer3:oma-1*. (**A**): *Cer3::oma-1* siRNA track plot for *oma-1* RNAi or control RNAi (L4440 empty vector) animals. dsRNA targeted region in *oma-1* is indicated. (**B**-**C**): RNA-seq MA-plots of *oma-1* RNAi vs control (L4440) RNAi and *oma-1* piRNAi vs control (*unc-119*) piRNAi, showing that both *oma-1* dsRNA and piRNA led to *oma-1* mRNA repression, but the dsRNA-triggered repression was weaker than the piRNA-triggered repression.

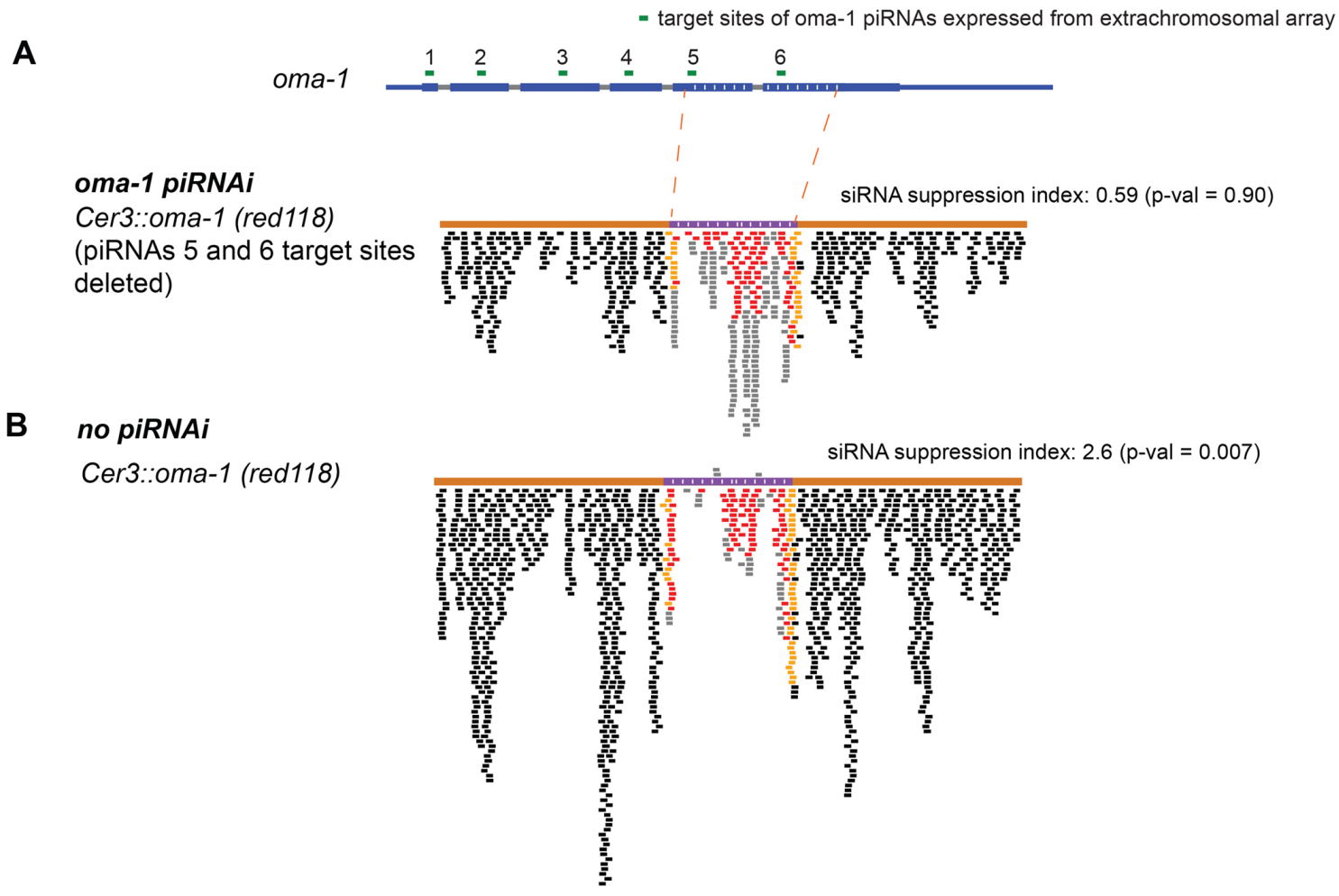

Fig. S6. Additional *oma-1* piRNAi experiments. The *oma-1* piRNAi transgene encodes six piRNAs. Their target sites in *oma-1* are indicated in (**A**). Two of the six piRNAs also target the *oma-1* fragment in *Cer3::oma-1* used in this study. To determine whether the effect of *oma-1* piRNAi on siRNA suppression was mediated by the piRNA target sites in the *Cer3::oma-1*, we generated a *Cer3::oma-1* allele (red118) that lacks these two target sites. The siRNA track plots with and without *oma-1* piRNAi are shown in **A** and **B**.

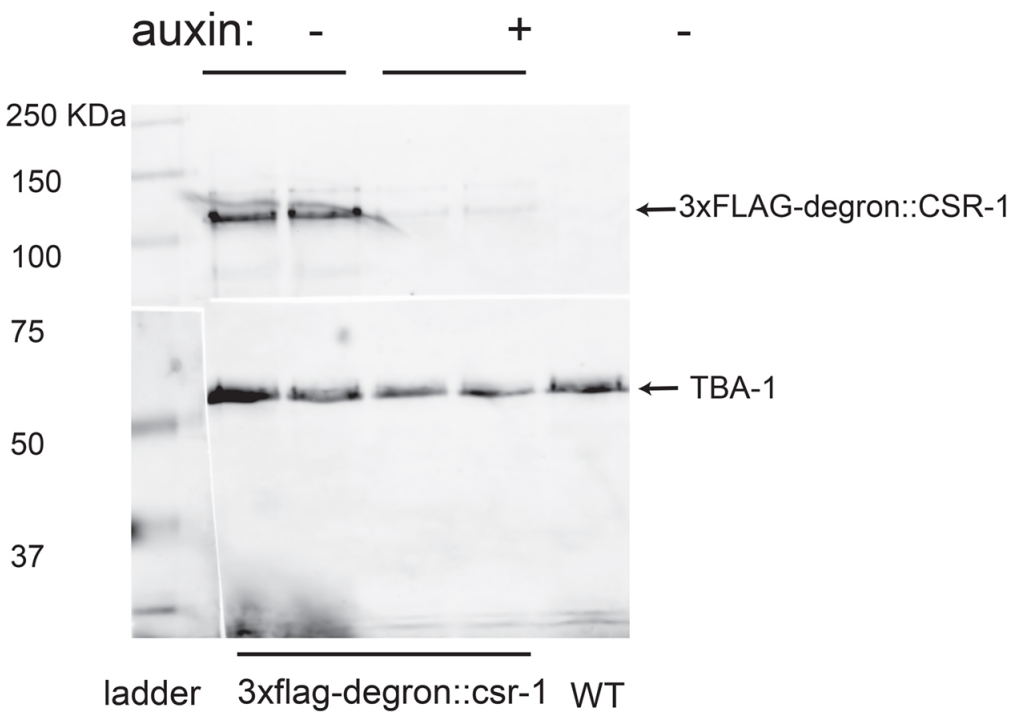

Fig. S7. Anti-FLAG western blot of 3xFLAG::degron::CSR-1 confirming auxin-induced degradation (AID) of CSR-1 (87% reduction). We note that, although the CSR-1 depletion was not complete, the animals exhibited a fully penetrant embryonic lethality, a phenotype expected for the loss-of-function *csr-1* mutation (data not shown).

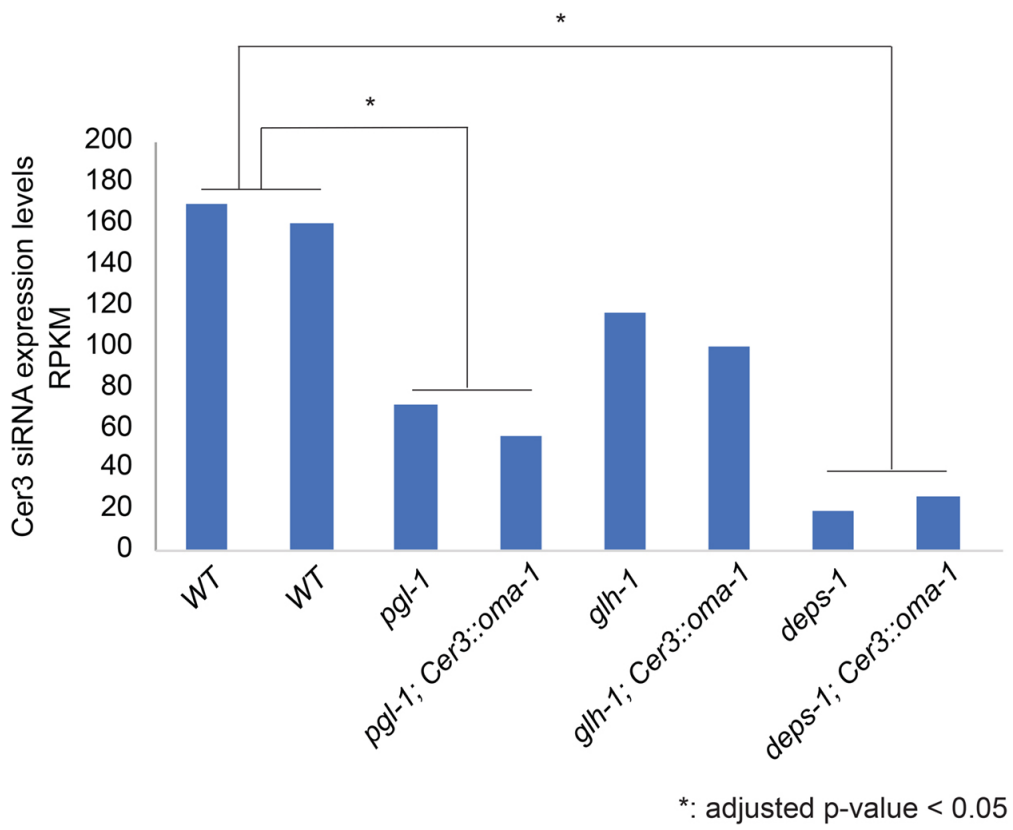

Fig. S8. *Cer3* siRNA expression levels in WT and P-granule mutant strains that carry either WT *Cer3* or *Cer3::oma-1*. The full-length WT *Cer3* sequence was used for the alignment to calculate the *Cer3* siRNA levels. DEseq2 (Love, Huber et al. 2014) was used to calculate the adjusted p-values for the comparison between WT and a mutant background. Both *pgl-1* and *deps-1* mutations were associated with significant reductions in *Cer3* siRNA production (3.7 and 9.2-fold reductions, respectively, adjusted p-values < $1.0x10^{-18}$). A modest *Cer3* siRNA reduction was observed in the *glh-1* mutant animals (1.7-fold, adjusted p-values = 0.2).

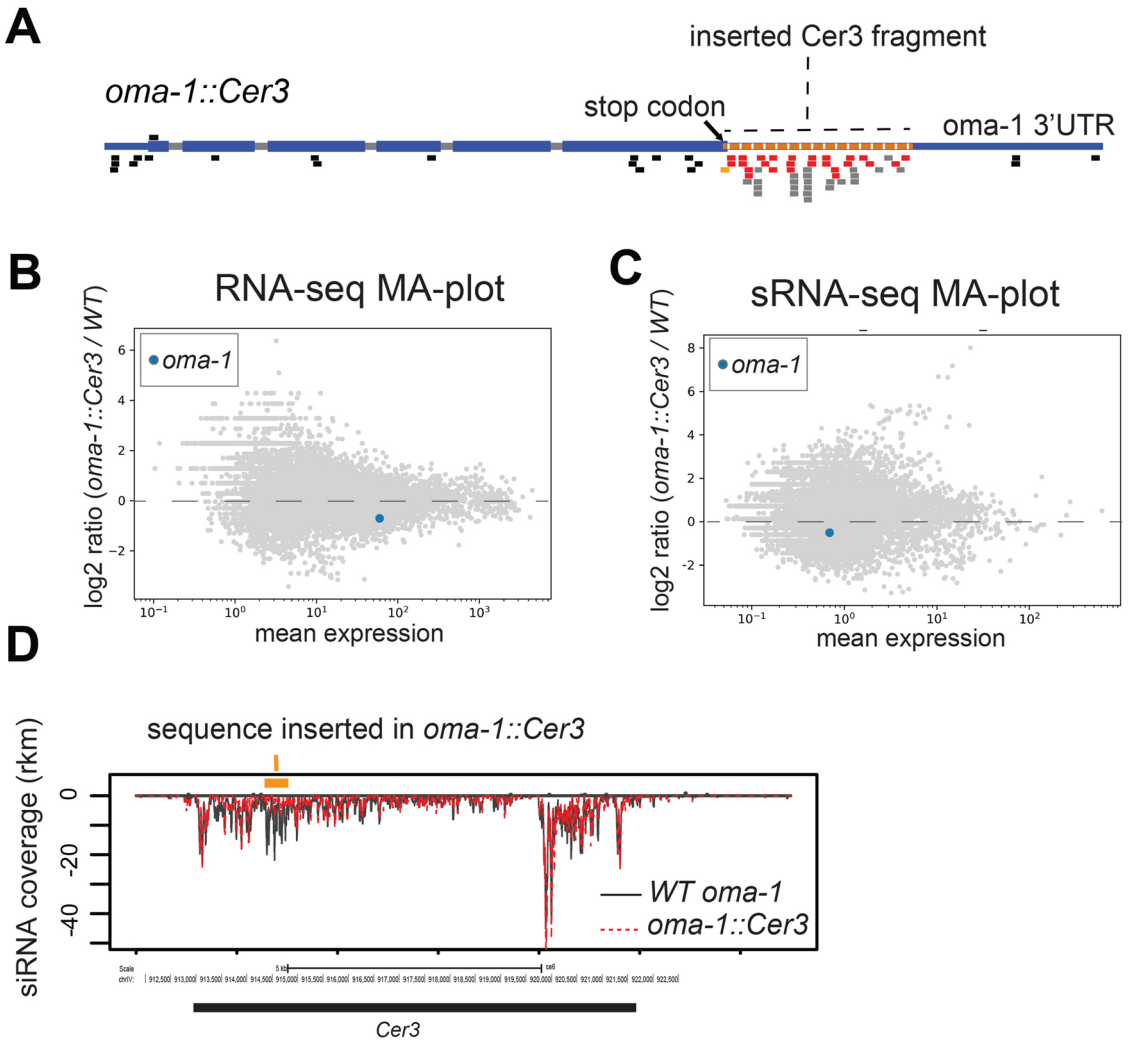

Fig. S9. Additional analysis for *oma-1::Cer3* mutant animals. (**A**) A track plot of *Cer3::oma-1* siRNA profile, with SNPs-containing siRNAs colored in red and siRNAs that do not cover any SNP position colored in gray. (**B-C**) MA-plots comparing *oma-1::Cer3* and WT mRNA (B) and siRNA (C) expressions for all genes, with *oma-1* highlighted in blue. The *Cer3* insertion was excluded from the analyses. (**D**) siRNA coverage plot at *Cer3*, normalized to the sequencing depth, for WT and *oma-1::*Cer3 animals using the same data as Fig. 5A and 5B.

Table S1. NGS libraries used in this study. All Fastq files have been deposited in NCBI with the GEO accession number GSE196847.

Click here to download Table S1